Scanning Electron Microscopy Studies of Nafion Deformation into Silicon Micro-Trenches for Fuel Cell Applications

Roxanne Schneider

April 15th, 2008

Professor Jay Benziger

Submitted in partial fulfillment of the requirements for the degree of Bachelor of Science in Engineering

Department of Chemical Engineering and Materials Science and Engineering Certificate Program

Princeton University

I hereby declare that I am the sole author of this thesis.

I authorize Princeton University to lend this thesis to other institutions or individuals for the purpose of scholarly research.

Roxanne Schneider

I further authorize Princeton University to reproduce this thesis by photocopying or by other means, in total or in part, at the request of other institutions or individuals for the purpose of scholarly research.

Roxanne Schneider

Princeton University requires the signatures of all persons using or photocopying this thesis. Please sign below and give address and date.

To my friends and family and everyone who has
helped make my life so exceedingly enjoyable.

Acknowledgements

I would like to begin by thanking all of the great teachers I have had over the years who helped spark my passion for math and science. I would also like to thank my parents for sacrificing to send me to the best schools possible.

I would like to thank Professor Benziger for allowing me to work under him and always having faith in my ability to work without direct supervision and clear my own path. I would also like to thank Professor Nan Yao for teaching such an elegant class on electron microscopy.

Thanks also go to Mikhail Gaevski, Professor Loo, and Professor Register for allowing me to use their respective facilities and labs. A special thank you goes to Joe Palmer for his words of wisdom and warm smile in the clean room, a place normally devoid of smiles.

I would like to thank Mr. James Inman and Mr. Roger Lee of the custodial staff of the Friend Center of Engineering. Their kind greetings and friendly faces were a constant reminder that even in the worst of times, life is good.

I would like to thank all of my dear friends at the Cap and Gown club, especially my roommates, and my twin sister Lizz for listening to me talk about my thesis even though I'm sure they all secretly found it exceedingly boring.

Last, but certainly not least, I would like to thank all of my classmates in the Chemical Engineering Department. Their camaraderie was undoubtedly the key to my simultaneous successful completion of the chemical engineering curriculum and retention of my sanity.

Abstract

Fuel cells are a potentially viable, clean, renewable source of energy. Polymer Electrolyte Membrane Fuel Cells (PEMFCs), which rely on the electrolyte copolymer Nafion, are particularly promising. It has been conjectured that the current output of a PEMFC is partially dependant on the degree to which the Nafion deforms into the catalyst layers at the electrodes of the fuel cell [1]. In 2005, Alison Lehr wrote her senior thesis on the temperature dependence of this interface and in 2007, Paul Majsztrik wrote about the interrelated ways temperature and hydration affect creep in Nafion. This thesis sought to fill the gap between the two works and study the way temperature and hydration synergistically affect the Nafion-catalyst interface. This thesis followed the Lehr procedure of creating an idealized model of the catalyst layer of a fuel cell by microfabricating 5μm deep trenches in silicon. Nafion was then pressed into the silicon at various temperatures and hydration levels. The samples were then freeze fractured and the resulting interface was viewed using a scanning electron microscope (SEM). This thesis concurred with the Lehr finding that as the temperature of the dry-pressed Nafion is increased, the deformation of Nafion into the trenches increases. This thesis also concurred with the Majsztrik finding that at 90^{o}C increasing hydration actually decreases deformation. It was also found that time, both the duration of applied pressure during pressing and the time allowed for relaxation between pressing and viewing, also affect the Nafion-silicon interface. Also, SEM damage observed during imaging indicated that Nafion undergoes some sort of microstructural rearrangement during deformation. These findings all have potential implications for the conditions of fuel cell fabrication and operation.

Table of Contents

Acknowledgements v
Abstract vi
Table of Contents vii
Table of Figures viii
1. Introduction 1
1.1 Motivation 1
1.2 Goals 4
2. Background 5
2.1 PEM Fuel Cell Basics 5
2.2 Nafion Structure and Function 7
2.3 Scanning Electron Microscopy 10
3. Experimental Procedure 11
3.1 Preparing and Spin Coating the Silicon Wafers 12
3.2 Patterning the Photoresist 13
3.3 Etching the Silicon Wafers and Completion of Microfabrication 14
3.4 Preparing the Nafion-Silicon Samples for Pressing 16
3.5 Freeze Fracturing and Preparation for the SEM 17
3.6 Imaging with the SEM
4. Results 19
4.1 The Hydration and Temperature Dependent Deformation of Nafion 19
4.1.1 Pressing at Ambient (27^{o}C) 19
4.1.2 Pressing at 50^{o}C 21
4.1.3 Pressing at 90^{o}C 24
4.1.4 Pressing at 120^{o}C 28
4.1.5 Pressing at 140^{o}C 29
4.2 Discussion of Temperature and Hydration Dependence of Deformation 30
4.3 Determining the Cause of the Discrepancy in Observation of Reverse Curvature 31
4.3.1 Testing the Effect of Pressure on Observed Curvature 31
4.3.2 Testing the Effect of Relaxation Time on the Nafion Features 33
4.4 The Effect of Pressing Time 37
4.5 Damage to the Nafion Due to SEM Imaging 39
5. Conclusion 45
5.1 Concurrence with the Majsztrik (2008) Study and Implications 45
5.2 Dissension from the Lehr (2005) Thesis and Implications 47
5.3 SEM Damage and Micro-structural Implications 47
5.4 Recommendations for Further Study 48
6. Reference 51

Table of Figures

Figure 1: Conjecture from Lehr 2004 illustrating that the delayed increase in current might be due to an increase in catalyst-Nafion contact area. [4] 3
Figure 2: Results of the Majsztrik 2007 dissertation showing that while increasing water activity levels leads to an increase in creep at low temperatures, the reverse relationship occurs at elevated temperatures. [5] 4
Figure 3: An illustration of the Nafion-catalyst interface in a fuel cell and the idealized model of this interface used in this thesis. 5
Figure 4: An illustration of the three-phase boundary at which the electrochemical reaction takes place in a PEM fuel cell. [1] 6
Figure 5: A schematic of a PEM fuel cell with a magnified view of the membrane-catalyst interface in the foreground. [1] 7
Figure 6: The chemical structure of Nafion where M^+ is the counter ion (H^+,Li^+, Na^+) . From Heitner-Wirguin (1996). [8] 8
Figure 7: The microstructure of Nafion according to Gierke's cluster-network model. From Heitner-Wirguin (1996). [8] 9
Figure 8: Illustration of Yeager and Steck's three region model of Nafion. Region A is the fluorocarbon, B is the interfacial zone, and C is the ionic clusters. Taken from Yeager and Steck (1981). [11] 10
Figures 9 A-C: An outline of the microfabrication process. 15
Figure 10: An illustration of the Nafion-silicon "sandwiches" prior to pressing. 16
Table 1: Temperature and water hydration of each round of pressing. 17
Figures 11 A-C: An illustration of the three types of SEM stage used. 18
Figure 12: A 650x magnified SEM image of the Nafion dry-pressed at 27°C. 20
Figure 13: A 3500x magnified SEM image of the Nafion wet-pressed at 27°C. 21
Figure 14: A 5000x magnified SEM image of the Nafion dry-pressed at 50°C 22
Figure 15: A 1500x magnified SEM image of the Nafion wet-pressed at 50°C 23
Figure 16: A 3500x magnified SEM image of the Nafion dry-pressed at 90°C. 24
Figure 17: A 2500x magnified SEM image of the Nafion dry-pressed at 90°C. 25
Figure 18: A 1000x magnified SEM image of the Nafion wet -pressed at 90°C. 26
Figure 19: An 800x magnified SEM image of the Nafion wet -pressed at 90°C. 27
Figure 20: A 5000x magnified SEM image of the Nafion dry-pressed at 120°C. 28
Figure 21: A 6500x magnified SEM image of the Nafion dry-pressed at 140°C 29
Figure 22: A 9158x magnified SEM image by Lehr (2005) of Nafion dry-pressed at 140°C. 29
Figure 23: An illustration of a) a crosslink between sulfonic groups in non-hydrated Nafion and b) a crosslink strengthen by a hydronium ion in hydrated Nafion. From Majsztrik 2007 [5]. 31
Figure 24: A 1500x magnified SEM image of the Nafion dry-pressed at 140°C with the same applied pressure as the Lehr 2005 thesis. 33
Figure 25: A 5000x magnified SEM image of the Nafion dry-pressed at 120°C. This image was taken approximately 6 hours after pressing. 34

Figure 26: A 3500x magnified SEM image of Nafion dry-pressed at 120°C. This image was taken of the same sample as the image to the left 28 days after pressing. 34
Figure 27: A simplified representation of the Nafion immediately after pressing and 28 days after pressing in this thesis and the Nafion in the Lehr thesis. 35
Figure 28: A 650x magnified SEM image of the Nafion dry-pressed at 25°C for one minute. 37
Figure 29: A 2000x magnified SEM image of the Nafion dry-pressed at 25°C for one hour. 37
Figure 30: A 5000x magnified SEM image of the Nafion dry-pressed at 50°C. 38
Figure 31: A 1000x magnified SEM image of the Nafion dry-pressed at 50°C for one hour. 38
Figure 32: 6,500x magnified SEM images of Nafion dry-pressed at 140°C. 40
Figure 33: A 5,000x SEM image of both the damaged and undamaged portions of a feature in the Nafion sample dry pressed at 140°C. 41
Figure 34: An illustration of the hypothetical restructuring of Nafion in the silicon trenches. 43
Figure 35: 1000x SEM images of Teflon that was dry-pressed into the silicon substrates at 120°C. The "Before" image shows the initial, unfocused image taken while the "After" image shows the focused image that was exposed to a 25keV incident electron beam for 10 minutes. 43
Figure 36: Graph from the 2007 Majsztrik [5] work and illustrations of the results of this thesis. 46

1. Introduction

1.1 Motivation

In the wake of concerns about global warming and a shortage of fossil fuels, a major focus in the scientific community has been research geared towards developing clean, renewable sources of energy. One such source of energy that neither directly relies on fossil fuels nor creates CO_2 as a byproduct is the fuel cell. While there are several types of fuel cell, polymer electrolyte membrane fuel cells (PEMFCs) are particularly promising because of their high power density, energy efficiency, and low operating temperature [1]. The fuel cell was discovered well over 100 years ago in 1839[1]. However, PEM fuel cells continue to be rigorously studied and there are many remaining questions that must be answered before these fuel cells become commercially viable. Much of the current research being performed on PEMFCs is geared toward developing control systems that can effectively keep fuel cells operating at the conditions that produce optimal output [2]. However, determining which parameters are optimal as set points in these control schemes is just as important as the control schemes themselves. The question therefore becomes: just what are the fabrication and operation conditions for optimal PEMFC power output and efficiency?

In 2004, Benziger et al.[3] modeled PEMFCs as two stirred tank reactors (STRs) and sought to understand the dynamic system output response to changes in operating parameters. After changing the resistive load on the fuel cell from 20Ω to 7Ω, an unusual multistep system response was observed. There was the expected jump in current initially following the decrease in load but there was also a completely unexpected second jump in current that occurred 1,500 seconds after the load change. With a decrease in load and the resulting increase in current, the fuel cell would produce more water, thus causing an increase in water activity level. The authors

conjectured that while the initial response of the fuel cell was due to a jump in current at constant water activity level, the later secondary response was due to changes in membrane properties stemming from this increase in water activity level.

In her 2005 senior thesis for the Princeton University Department of Chemical Engineering, Alison Lehr [4] proposed that the increase in water production associated with the initial jump in current caused the Nafion membrane to swell and deform into the porous catalyst layers present at the electrodes. As illustrated in figure1, this increase in contact area between the membrane and the catalyst particles would result in an increase in the rates of the reactions taking place at the electrodes and would explain the secondary increase in current observed by Benziger et al., 2004. Lehr sought to better understand the conditions at which Nafion would deform furthest into the catalyst layer. She modeled the catalyst layer as a series of trenches in silicon. She then pressed Nafion into the trenches at various temperatures and viewed the resulting Nafion-silicon interface with a Scanning Electron Microscope (SEM). Lehr found that, in general, as the temperature of pressing increased, the deformation of the Nafion into the silicon substrate also increased. She also found that below 140^{o}C, Nafion deformed into the trenches in a single peak manner in which the Nafion did not wet the sides of the trenches, whereas above 140^{o}C, Nafion deformed into the substrate in a two peak manner in which the Nafion did wet the sides of the trenches.

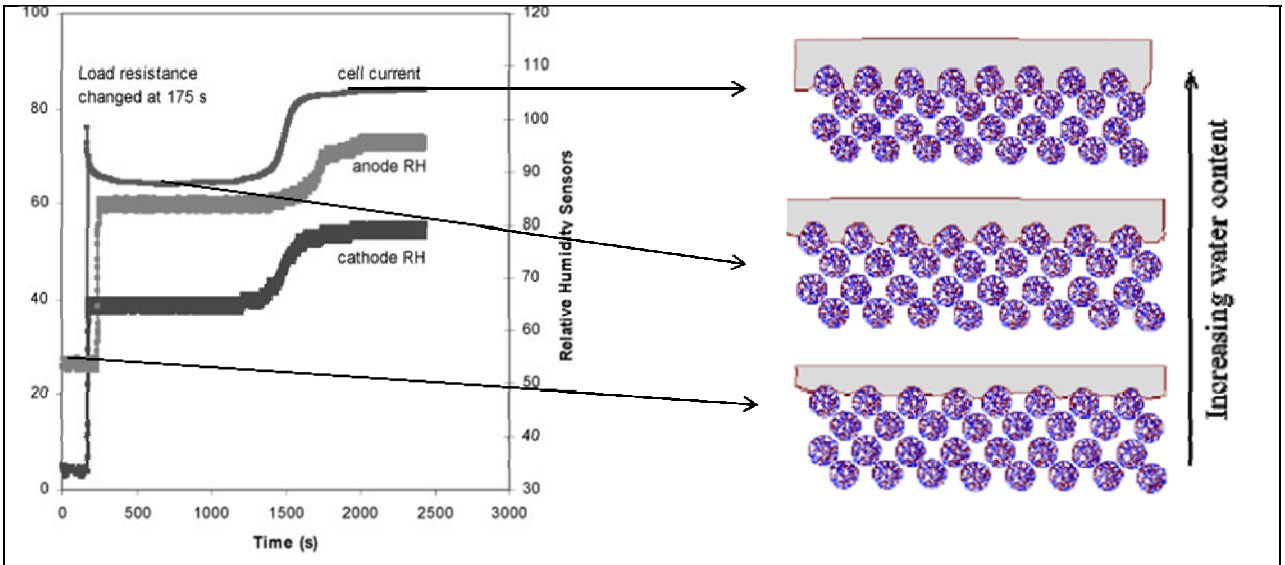

Figure 1: Conjecture from Lehr 2004 illustrating that the delayed increase in current might be due to an increase in catalyst-Nafion contact area. [4]

In his 2007 dissertation work, Majsztrik investigated creep rates of Nafion at different temperatures and water activity levels [5]. Creep is the deformation of a material caused by exposure to a stress for an extended period of time [6]. Creep would therefore affect deformation of Nafion into a catalyst layer if pressed for a prolonged period of time. As shown in figure 2, the Majsztrik work found that at room temperature, an increase in water activity level was associated with higher rates of creep, while at 90^{o}C the reverse relationship was observed. While Lehr was not able to investigate the relationship between water activity level and deformation, the Majsztrik dissertation shows that the nature of the deformation of Nafion in relation to temperature and water activity level is complicated. The work done by Benziger at al. (2004) shows that understanding this relationship and the way it affects the Nafion-catalyst interface is critical to understanding the optimal conditions of fuel cell fabrication and operation.

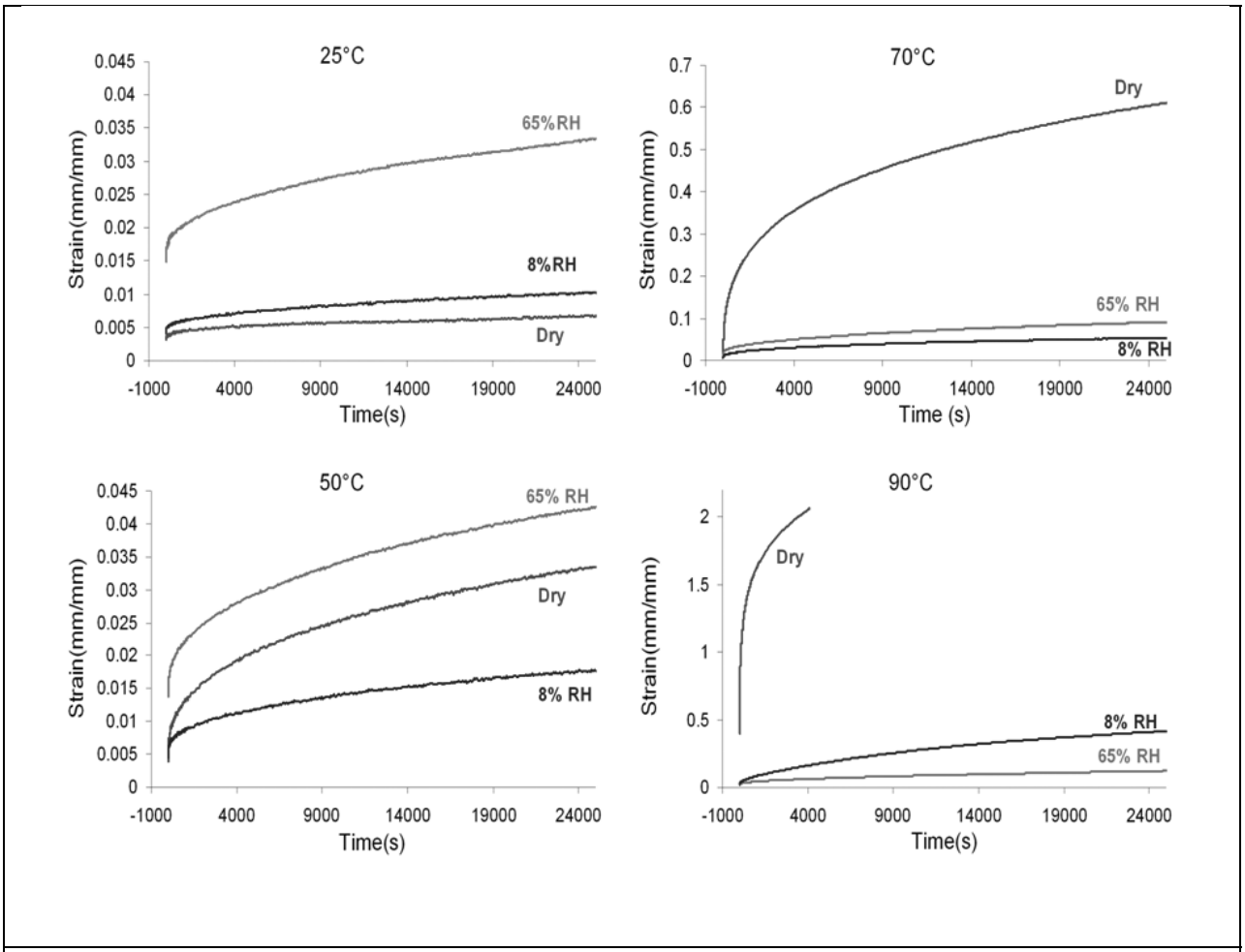

Figure 2: Results of the Majsztrik 2007 dissertation showing that while increasing water activity levels leads to an increase in creep at low temperatures, the reverse relationship occurs at elevated temperatures. [5]

1.2 Goals

This thesis examines the way temperature, water activity level, and time affect the Nafion-catalyst interface in a PEM fuel cell. As illustrated in figure 3, the catalyst layer is modeled by a silicon substrate microfabricated such that it has 5μm deep trenches that vary between 2 and 20μm wide. Both wet and dry Nafion are pressed into the silicon substrates at various temperatures to simulate the manufacturing process of a PEM fuel cell. The substrates are freeze fractured and the resulting Nafion-silicon interfaces are observed using a Scanning

Electron Microscope (SEM). Theoretically, the further the Nafion deforms into the silicon trenches, the greater the Nafion-catalyst contact area would be, potentially leading to a more fuel cell with higher current output.

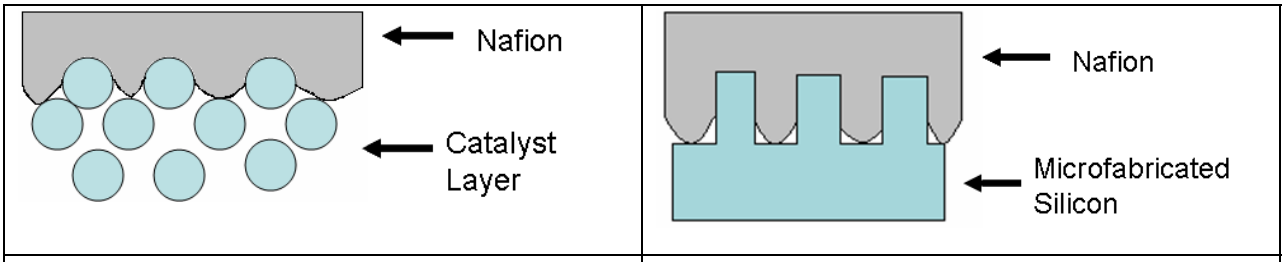

In a Fuel Cell	Idealized Model

Figure 3: An illustration of the Nafion-catalyst interface in a fuel cell and the idealized model of this interface used in this thesis.

2 Background

2.1 PEM Fuel Cell Basics

A fuel cell is a device that is capable of converting chemical energy into electric energy [1]. The basic components of a fuel cell are an anode which is in contact with the fuel, a cathode which is contact with the oxidant, and an electrolyte which separates these two electrodes [1]. These basic components and their ability to generate electricity from electrochemical reactions draw an immediate comparison between fuel cells and traditional batteries. However, fuel cells are different from batteries in several key aspects. In batteries, the materials that undergo reactions must be internally stored, which means that the life of a battery is limited by the depletion of these materials. In a fuel cell, both the fuel and oxidant are fed in from an external source meaning that the fuel cell will never be discharged as long as these two reactants are

continuously supplied [1]. The typical fuel for a fuel cell is hydrogen and the typical oxidant is oxygen but the form in which these substances are used is dependent on the type of fuel cell.

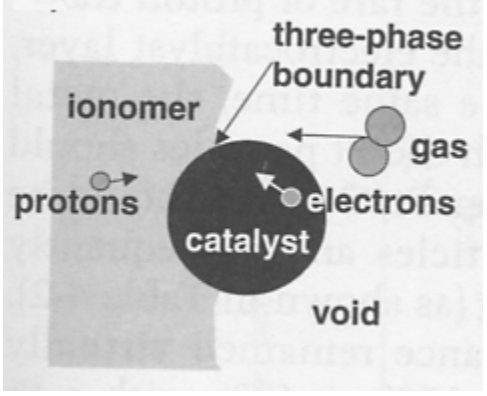

Figure 4: An illustration of the three-phase boundary at which the electrochemical reaction takes place in a PEM fuel cell. [1]

It is the PEM fuel cell that shows the most promise for commercial viability because of its simplicity, useful temperature range, and quick start up [1]. Polymer electrolyte fuel cells (PEMFCs), also referred to as proton exchange membrane fuel cells, use a proton conductive polymer membrane as the electrolyte. In a PEMFC, the membrane, which must also be impermeable to gases, is pressed between the two electrodes. At the interface between the electrodes and the membrane is a catalyst layer typically comprised of platinum supported on carbon [1]. As can be seen in figure 4, the electrochemical reaction occurs at the three-phase boundary between the membrane, the feed gas, and the catalyst. It is during this reaction that hydrogen is split into protons and electrons. Figure 5 outlines the basic processes that take place within a fuel cell. The protons travel through the membrane to the cathode while the electrons travel from the anode, through current collectors, and through outside circuits where the current they generate performs work [1]. The electrons then travel to the cathode on the opposite end of the fuel cell, where they meet with the protons and oxygen, producing water that is ultimately pushed out of the cell by excess oxygen. The result of these reactions and transport processes is the flow of electrons through an external circuit, direct electrical current [1]. One of the limiting factors for the rate at which this process takes place, and therefore the current output of the fuel

cell, is the area of the three-phase boundary at which the electrochemical reaction takes place. The degree of contact between the membrane and the catalyst layer is therefore very important to the overall output of the fuel cell and it is the nature of this membrane-catalyst interface that will be examined in this thesis.

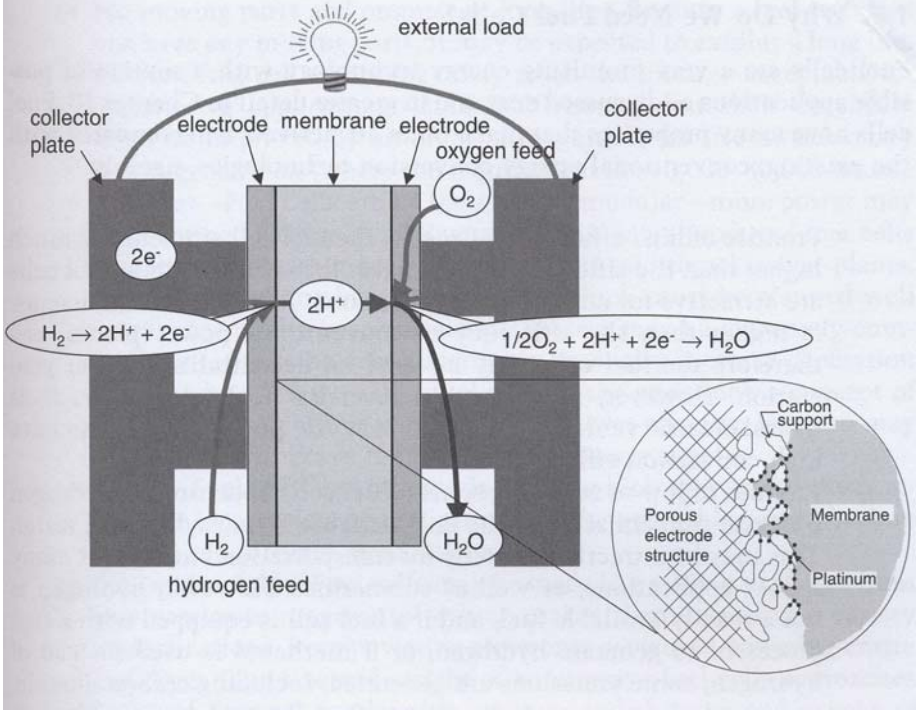

Figure 5: A schematic of a PEM fuel cell with a magnified view of the membrane-catalyst interface in the foreground. [1]

2.2 Nafion: Structure and Function

With the knowledge of how a fuel cell works it is apparent that the membrane used in a PEM fuel cell must be very highly proton conductive and yet also be impermeable to the fuel and reactant gases. In addition to these constraints on the membrane material, it must also be chemically and mechanically resistant to damage under the operating conditions of the fuel cell

[1]. Perfluorocarbon-sulfonic acid ionomers (PSA) are one of the few substances that meet these requirements and are the most widely used membranes in fuel cells [7]. PSA is a copolymer of tetrafluorethylene (TFE) and various perfluorosulfonate monomers. Nafion, which is manufactured by Dupont, is perhaps the most widely known and researched PSA and is composed of perfluoro-sulfonylfluoride ethyl-propyl-vinyl ether (PSEPVE) [7]. Figure 6 shows the chemical structure of Nafion.

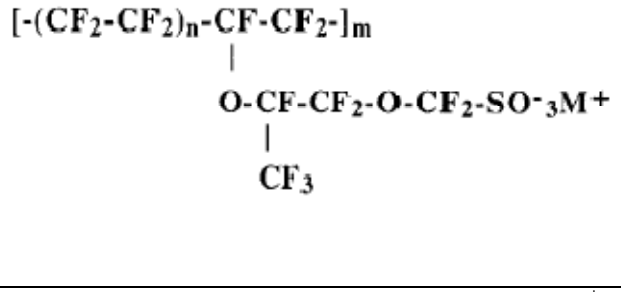

Figure 6: The chemical structure of Nafion where M^+ is the counter ion (H^+,Li^+, Na^+) . From Heitner-Wirguin (1996). [8]

The SO_3H group is actually ionically bound together and the side chain of Nafion is therefore terminated by SO_3^- and H^+ ions [8]. The resulting structure of Nafion is such that the sulfonic acid groups are highly hydrophilic while the TFE backbone is highly hydrophobic. These hydrophilic regions are the reason that Nafion is able to absorb relatively large amounts of water. Using small angle x-ray scattering and dynamic mechanical analysis, Yeo and Eisenberg in 1977 [9] were the first to propose that because of this dissimilarity in hyrdophobicity, the sulfonic acid groups tend to cluster together creating hydrophilic regions within the bulk of the Nafion. In 1981, Gierke [10] similarly used small angle x-ray scattering and wide angle x-ray diffraction to refine this cluster-network model of Nafion. As illustrated in figure 7, in the Gierke cluster-network model, aqueous ions form clusters that are connected by narrow channels. The water content of the Nafion varies the size of the clusters and channels, which in turn determine the

transport properties of the membrane. Gierke asserted that Nafion's proton conductivity stems from the ability of H^+ ions to move along these hydrated regions.

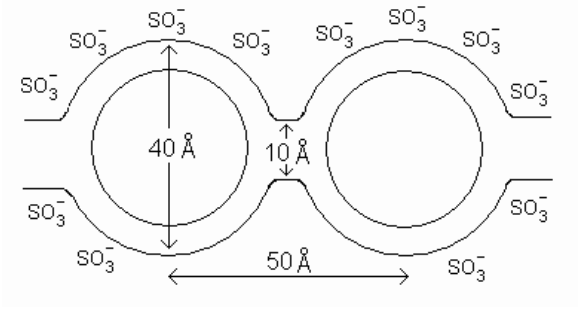

Figure 7: The microstructure of Nafion according to Gierke's cluster-network model. From Heitner-Wirguin (1996). [8]

Also published in 1981 was a work by Yeager and Steck [11] which studied self diffusion coefficients of sodium, cesium, and water in Nafion. From the results of this study, they concluded that hydrated Nafion was comprised of three distinct regions as illustrated in figure 8. Region A is the fluorocarbon backbone, TFE. Region B is the interfacial zone containing mostly void space with some side chain material and small amounts of water and sulfonate exchange sites. Similar to the Gierke model, Yeager and Steck proposed that region B provides a continuous diffusion path among ion clusters. Both models suggest that the transport of hydrogen that is so crucial to the function of a fuel cell occurs by transport between and within hydrophilic clusters. Both models also assert that the microstructure of Nafion is greatly affected by both water activity level and temperature. This thesis will attempt to determine if and how macroscopic structural changes are resultant of these micro-structural changes due to temperature and water activity level.

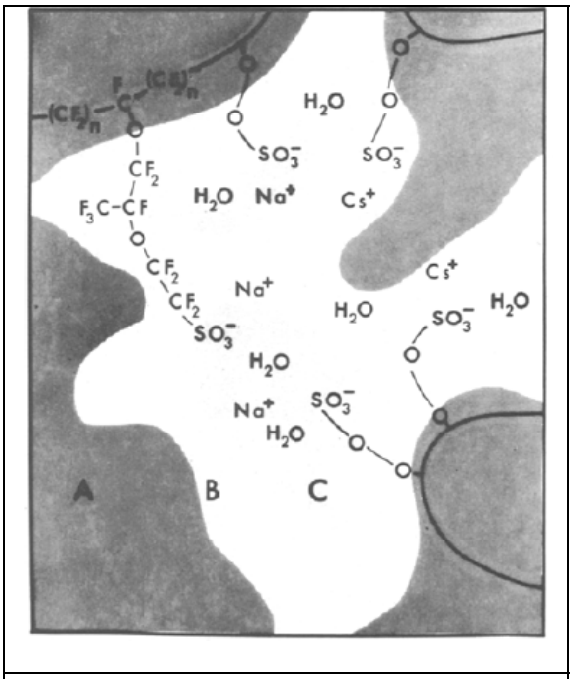

Figure 8: Illustration of Yeager and Steck's three region model of Nafion. Region A is the fluorocarbon, B is the interfacial zone, and C is the ionic clusters. Taken from Yeager and Steck (1981). [11]

2.3 Scanning Electron Microscopy

While optical microscopy is the simplest and least expensive small-scale materials characterization technique, optical microscopy is limited in its resolution by the wavelength of light. The visible light used in optical microscopes has wavelengths varying between 400 and 700 nanometers [12]. With the presence of spherical aberration, these wavelengths translate into a resolution of one to two micrometers in most optical microscopes [12]. A scanning electron microscope (SEM) uses electrons rather than light to generate images and the resolution of an SEM is therefore limited by the wavelength of electrons, which at the standard energy of 5keV is only .55 nm [13]. With the presence of other limiting factors, again such as lens aberration, the ultimate resolution power of a 5keV SEM is on the order of a few nanometers [13]. The features that need to be imaged in this study are a few micrometers in width, making them slightly too small to be accurately resolved with an optical microscope. Instead, the improved resolution of an SEM was needed to generate useful images.

A scanning electron microscope works by focusing a source of electrons into a fine point that can be scanned over the surface of the object being viewed [13]. When the scanning electrons hit the surface of the material being imaged, several interactions occur. In this thesis,

all of the images were generated by collecting secondary electrons, electrons from the material being imaged that get knocked off by the incident electron beam. The secondary electrons are collected by a detector where information from the electrons is used to form an image of the material being viewed [13]. In this way, the SEM provides a highly magnified image of the surface of a material that is very similar to what one would "see" if optical imaging were possible on such a small length scale.

It is important to bear in mind that while similar, SEM images are not optically generated and that the SEM images might have subtle differences that could potentially be misleading. For example, in an SEM the brightness of an area in an image is dependant on the number of secondary electrons reaching the detector from that area [13]. While this is the reason that SEMs are able to generate sharp, three-dimensional images, it can also lead to an "edge effect" in which sharp edges of a sample appear abnormally brighter than the rest of the sample. Also, it is important to note than unlike an optical microscope, imaging in an SEM can lead to sample damage. The interaction between the incident electron beam and the sample can often be destructive to the material being viewed [14]. As will be seen later on, the way in which sample damage occurs can occasionally be used to gather information on the nature of the material being viewed.

3. Experimental Procedure

In order to create the silicon substrates with 5μm deep trenches between 2μm and 20μm wide, microfabrication techniques needed to be employed. Microfabrication of the substrates

was performed under clean room conditions to avoid contaminating the desired surface topography with dust and various other micron-sized particulate matter present in the air. The silicon wafers were cleaned and spin coated in the PRISM clean room of Princeton University and then transported to the clean room of Professor Loo of Princeton University's Department of Chemical Engineering, where they were exposed and developed. The resulting substrates were then transported back to the PRISM clean room to be etched and cleaned. Nafion was then pressed into the etched silicon wafers using a heated polymer press, after which the samples were freeze fractured and viewed with the Scanning Electron Microscope in Princeton's Imaging and Analysis Center.

3.1 Preparing and Spin Coating the Silicon Wafers

The silicon used was p-type doped, 380±20 μm thick, and polished on one side. The silicon wafers were initially 3 inches in diameter. However, the large size of the wafers made obtaining a uniform layer of photoresist difficult. In order to consistently obtain wafers that were covered by photoresist of a uniform thickness, the wafers were fractured into quarters.

Each silicon "wedge" shaped section was then blown with clean, dry nitrogen in order to remove any dust that might have been created during the fracturing process. Each silicon section needed to be cleaned by rinsing in acetone for several seconds, drying with N_2, rinsing with methanol, drying with N_2, and then rinsing with isopropyl alcohol and finally drying with N_2 again. Cleaned silicon was heated at 110^{o}C on a hotplate for at least 15 minutes in order to completely dehydrate the samples.

After dehydration, each silicon substrate was spin coated with a layer of Hexamethyldisilazane (HMDS) at 4,000 rpm for 40 seconds in order to help the subsequently

applied photoresist adhere to the silicon. A layer of AZ5214 photoresist was then spin coated onto the silicon, again at 4,000 rpm for 40 seconds. After application of the photoresist, each substrate was then softbaked on a hotplate at 90^{o}C for 60 seconds. Softbaking improves the adherence of the photoresist to the silicon wafer.

3.2 Patterning the Photoresist

After this application of the photoresist, each substrate was exposed through a mask to UV light with a power of 2.0mW/cm^2 for 45 seconds. The direct contact method of exposure in which the mask is placed directly on the substrate was used in order to obtain the highest resolution possible and because of the method's relative ease. For consistency, the mask used was the same mask created and used by Alison Lehr in her 2004 work. The photoresist employed, AZ5214, is a positive photoresist and therefore becomes chemically less stable when exposed to UV light, allowing the exposed portion of the photoresist to later be removed while leaving the non-exposed portions intact. The mask used to cover the silicon substrate during exposure was thus a darkfield mask, meaning that the UV light was only allowed to penetrate in areas where trenches were ultimately desired.

It is interesting to note that great care needed to be taken to cover the spin coated samples to protect them from exposure to both sunlight and artificial light when transporting the spin-coated samples between labs. Initial attempts at the photolithographic process were thwarted due to unknown exposure to ambient UV rays during transportation.

After exposure, the substrates were submerged and continuously agitated in a 50:50 mixture of MIF312 developer and deionized water for 35 seconds. Upon removal from the developer, each substrate was rinsed with deionized water for 60 seconds and then viewed under

an optical microscope to ensure that the correct pattern was accurately present in the photoresist. The most frequent problems that were present in the patterning were dust that was present on the substrate due to failure to employ proper clean room technique and photoresist of a non-uniform thickness that resulted from improper spin coating. Substrates that were not correctly patterned were rinsed in acetone, methanol, and isopropyl alcohol to strip the silicon of all photoresist. Correctly patterned substrates were hardbaked by heating them on a hotplate for 6 minutes at 110^{o}C. During the hardbaking step a portion of the solvents present in the photoresist evaporate, leaving the resist harder and denser, ultimately providing better adhesion to the silicon.

3.3 Etching the Silicon Wafers and Completion of Microfabrication

After hard baking, the substrates were reactive ion etched in the Plasmatherm 720. In reactive ion etching, gases are fed into a chamber containing the substrate and a strong radio frequency electromagnetic field is applied [15]. The electric field ionizes the gases in the chamber by stripping them of electrons, resulting in a plasma of positively charged gas ions and fast moving electrons. As illustrated in figure 9A, a negative charge develops on the wafer as electrons collide with it and eventually the charge is large enough to draw the more massive gas ions to collide with the wafer [15]. It is this collision that is ultimately responsible for the removal of silicon and the creation of the desired surface topography as only exposed silicon, not silicon covered with photoresist, gets removed during the reactive ion etching process.

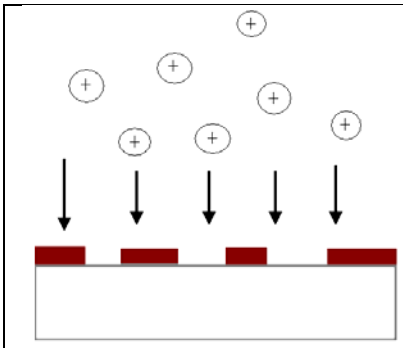

Figure 9A

Figure 9B

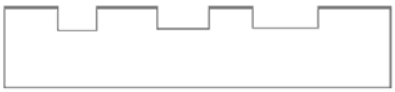

Figure 9C

Figures 9 A-C: An outline of the microfabrication process. Figure A shows the reactive ion etching process in which gas ions collide with the silicon substrate. Only the exposed silicon is etched away resulting in Figure B. After the remaining photoresist is removed, microfabrication is complete resulting in Figure C, ready to be pressed with Nafion.

The recipe followed during reactive ion etching was provided by the PRISM clean room at Princeton University. The pressure and temperature in the chamber were 100mTorr and 25^{o}C. The gasses used were SF_6 and CCl_2F_2 at flow rates of 60 and 20 sccm respectively. The power used was 100W and the total etch time was 25 minutes resulting in trenches in the silicon that were approximately 5 μm deep. Subsequently attempting to remove the photoresist with several different solvents, it was found that ethyl alcohol was most effective. In order to remove the photoresist, each substrate was soaked in boiling ethyl alcohol for approximately ten minutes and then scrubbed, while submerged in ethyl alcohol, with cotton tipped swabs. The substrates were cleaned a final time by again rinsing in acetone, methanol, and isopropyl alcohol and drying with dry nitrogen. The depth of the trenches was checked by using a profilometer.

3.4 Preparing the Nafion-Silicon Samples for Pressing

The Nafion pressed into the etched wafers was Nafion 1110, with a thickness of approximately 250 μm. The Nafion was prepared in order to both clean the polymer of any undesired particles and residues and also to ensure that it was correctly ionized. The Nafion was boiled for one hour in hydrogen peroxide (H_2O_2) and then boiled in deionized water for twenty minutes. The Nafion was then boiled in 1M sulfuric acid (H_2SO_4) for an additional hour before boiling it again in deionized water for twenty minutes. The cleaned pieces of Nafion were dried between filter paper and stored in a standard "Zip-Lock" bag.

In clean room conditions, the Nafion was then cut into 1 in. by .5 in. sections and placed on top of the pattern of trenches that had been etched in the silicon. Blank, non-etched silicon was then cut to the same dimensions as the etched pieces were placed on top of the Nafion, creating a silicon-Nafion "sandwich" as illustrated in figure 10.

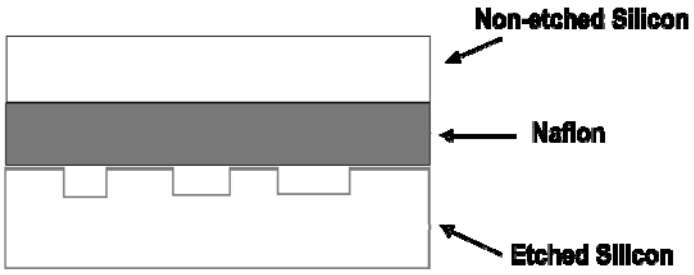

Figure 10: An illustration of the Nafion-silicon "sandwiches" prior to pressing. Note that the figure is not drawn to scale.

The resulting Nafion-silicon "sandwiches" were pressed using a heated polymer press. Each sample was pressed at one of the pressing conditions outlined in table 1. Initially, all of the sandwiches were pressed for 60 seconds in order to replicate the conditions of pressing used in the Lehr thesis. In a second round of testing, a few select samples were pressed for one hour in order to understand the effect of creep on the Nafion-silicon interface.

The samples that were "dry- pressed" were pressed in air at ambient relative humidity. The dry Nafion-silicon sandwiches were given ample time on the heated press prior to pressing so that the entire sample equilibrated at the desired temperature. The Nafion pieces that were "wet- pressed" were heated to the pressing temperature in water while the press itself was also heated to the pressing temperature. The Nafion was then transported from the water bath to the press immediately prior to pressing. After pressing, the samples were left in an oven at 90^{o}C and 0% relative humidity overnight to simulate "operating conditions" of a fuel cell and to ensure that the wet-presses samples dehydrated enough to be imaged in the scanning electron microscope. Note that normal operating conditions of a fuel cell would have had the Nafion more hydrated than the 0% relative humidity allowed.

Table 1: Temperature and water hydration of each round of pressing.

Temperature (^{o}C)	Wet/Dry
25	Wet
50	Wet
90	Wet
120	Dry
140	Dry
25	Dry
50	Dry
90	Dry

3.5 Freeze Fracturing and Preparation for the SEM

The pressed samples were removed from the oven and submerged in liquid nitrogen for approximately one minute. They were then removed from the liquid nitrogen using tweezers and notches were made on both sides of the silicon using a diamond scribe. The samples were then snapped in half by hand (while wearing protective gloves) such that cross sections of the trenches were exposed. The resulting sections of the silicon-Nafion substrates sandwiches were then trimmed by more fracturing. It was extremely difficult to fracture the substrates correctly in

order to produce an interface that could be adequately viewed. Very often, the silicon did not remain in contact with the Nafion after the freeze fracturing process. This subsequently led to the need to remake many of the samples and start over. Also, this difficulty in fracturing occasionally made viewing the interface itself impossible. In these cases, images of the Nafion alone were used to gather information on the deformation of the Nafion.

3.6 Imaging with the SEM

Prior to viewing in the SEM, the samples were sputter coated in the VCR IBS/TM 200S Ion Beam Sputterer in the PRISM Imaging and Analysis Center. Samples are sputter coated in order to make their surfaces more conductive and therefore less susceptible to the accumulation of surface charge. The samples were then attached to the appropriate SEM stages using carbon tape. The samples in which the Nafion and silicon remained intact produced the best images of the interface and were attached to 45^{o} angled SEM stages as shown in figure11B.

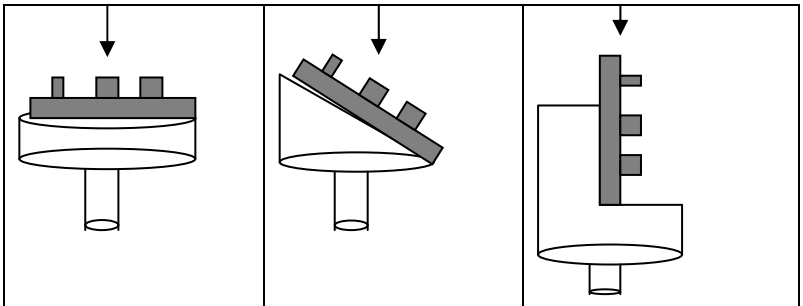

Figure 11A	Figure 11B	Figure 11C

Figures 11 A-C: An illustration of the three types of SEM stage used. Note that the arrow indicates the direction of the incident electron bream. Figures 11 A,B,andC respectively show the 0,45 and 90 degree stages used. Note that the image is not drawn to scale and in actuality the Nafion samples were significantly smaller than the stages themselves.

With many samples, the silicon did not remain in contact with the Nafion after the fracturing process, which resulted in the lack of a true interfacial cross section available for viewing. In samples in which the silicon broke away from the Nafion, the pieces of the Nafion

alone were carbon taped to both 0^o and 90^o SEM stages. The 90^o stages shown in figure 11C produced images of the cross section of the Nafion, however, these images often revealed little useful information about the nature of the silicon-Nafion interface. The 90^o stages produced images of the edges of the Nafion that were produced during fracturing, which were often deformed by the fracturing process. The 0^o stages shown in image 11A produced "birds eye view" images of the samples which provided information on whether or not the Nafion had deformed into the silicon trenches but did not show the height of any aspects of Nafion's topography and thus failed to show the degree to which the Nafion filled the silicon trenches.

4. Results

4.1 The Hydration and Temperature Dependent Deformation of Nafion

4.1.1 Pressing at Ambient (27^oC)

Dry-Pressed

The Nafion pressed at 25^oC did not show evidence of flow into the silicon trenches. Figure 12 shows that while the Nafion did deform somewhat and shows a mild outline of the silicon trenches, there was no significant flow and the Nafion did not effectively fill the trenches. It is interesting to note the presence of striations in the Nafion, most likely due to the stress the Nafion endured during pressing.

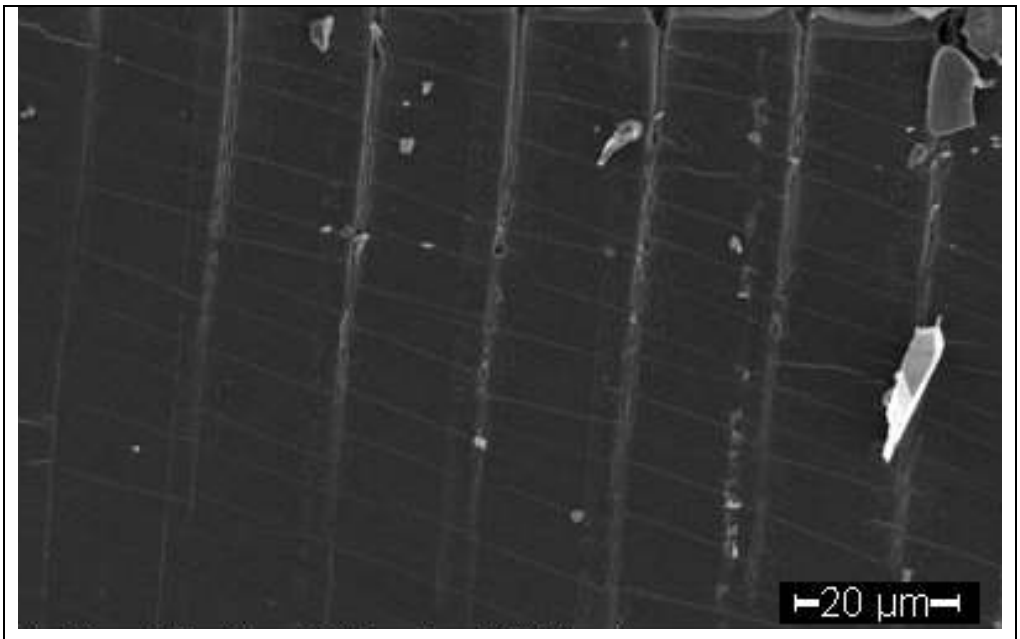

Figure 12: A 650x magnified SEM image of the Nafion dry-pressed at 27°C. Note that only a slight outline of the silicon trenches (vertical lines) is visible, indicating mild deformation. Also note the presence of striations (horizontal pattern) most probably due to the stress on the Nafion during pressing.

Wet-Pressed

As can be seen in figure 13, the sample wet-pressed at 27°C shows key similarities to the sample pressed dry at 27°C. Luckily, with this sample the silicon remained in contact with the Nafion, allowing for the imaging of the silicon-Nafion interface. In figure 13, the silicon substrate is at the top of the image while the Nafion is at the bottom of the image. The image shows that under these conditions, the Nafion failed to deform into the trenches yet shows a mild outline of the silicon features just as was the result in the dry-pressed case. Also, the same orthogonal striations present in the dry pressed Nafion are also present in the Nafion wet pressed at 27°C.

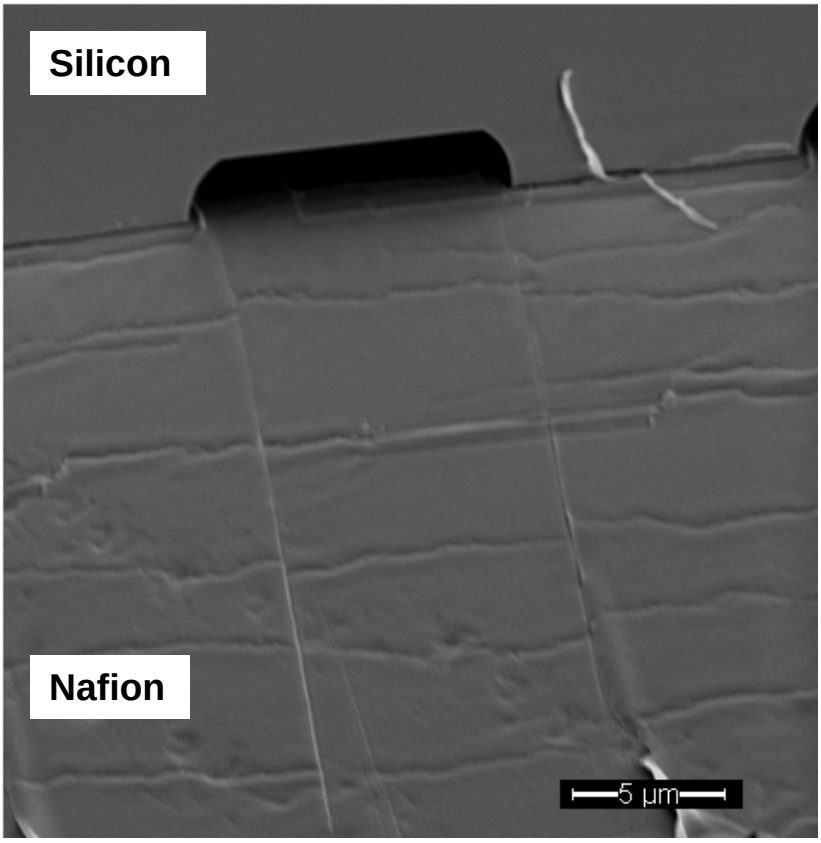

Figure 13: A 3500x magnified SEM image of the Nafion wet-pressed at 27°C. Note that only a slight outline of the silicon trenches (vertical lines) is visible, indicating only very slight deformation. Also note the presence of the same orthogonal striations as observed in the 27°C dry-pressed sample.

4.1.2 Pressing at 50°C

Dry-Pressed

The Nafion pressed at 50°C does appear to have partially deformed into the silicon trenches. While the Nafion and the silicon have shifted slightly away from each during the freeze fracturing process, figure 14 shows that the Nafion that was dry-pressed into the silicon at 50°C clearly has retained the pattern of the trenches. As can be seen by the silicon particle that has broken off into the trench in the upper right hand corner of the image, the features in the

Nafion are not very deep. The shallowness of the Nafion features indicates that during pressing the Nafion deformed only partially into the silicon trenches. It is interesting to note that there are only minor striations present in the Nafion dry-pressed at 50°C.

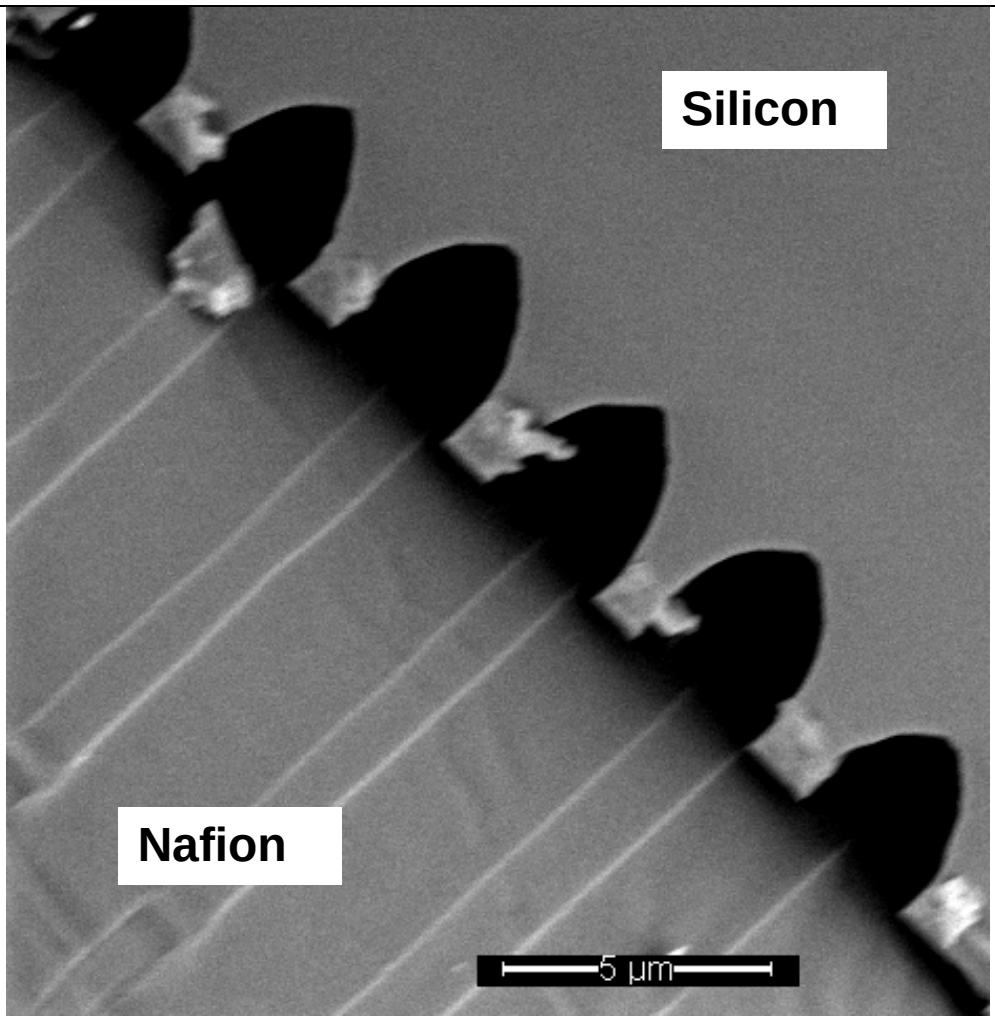

Figure 14: A 5000x magnified SEM image of the Nafion dry-pressed at 50°C. The silicon and Nafion have shifted slightly away from each other during the freeze fracturing process. It can still be seen that the outline of the trenches is present in the Nafion. As can be seen by the silicon particle that has broken off into the trench in the upper right hand corner, the features in the Nafion are not very deep and thus indicate only partial deformation into the silicon trenches.

Wet-Pressed

Figure 15 shows an image of the Nafion wet-pressed at 50°C. While it is again difficult to tell the exact height to which the Nafion deformed into the silicon trenches, the resulting

features appear to be similar to those in the Nafion dry-pressed at 50°C. As can be seen by observing the silicon particle in the center of the image that has broken off and lies across imprints in the Nafion, the features in the Nafion are again very shallow. This indicates that similar to the Nafion dry-pressed at 50°C, the Nafion wet-pressed at 50°C penetrated only negligibly into the silicon trenches. It is interesting to note the lack of striations in the Nafion wet-pressed at 50°C.

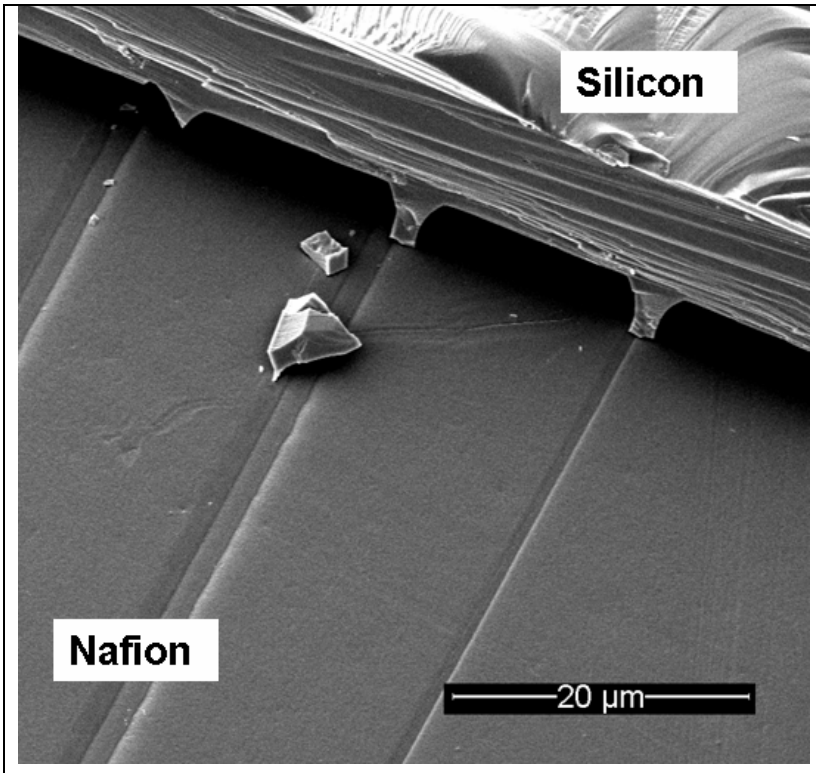

Figure 15: A 1500x magnified SEM image of the Nafion wet-pressed at 50°C. Note that the Nafion seems to have shifted by about 1 micron during sample preparation but it is still clear that while the Nafion has deformed into the outline of the silicon trenches, it has not significantly penetrated into the trenches.

4.1.3 Pressing at 90°C

Dry-Pressed

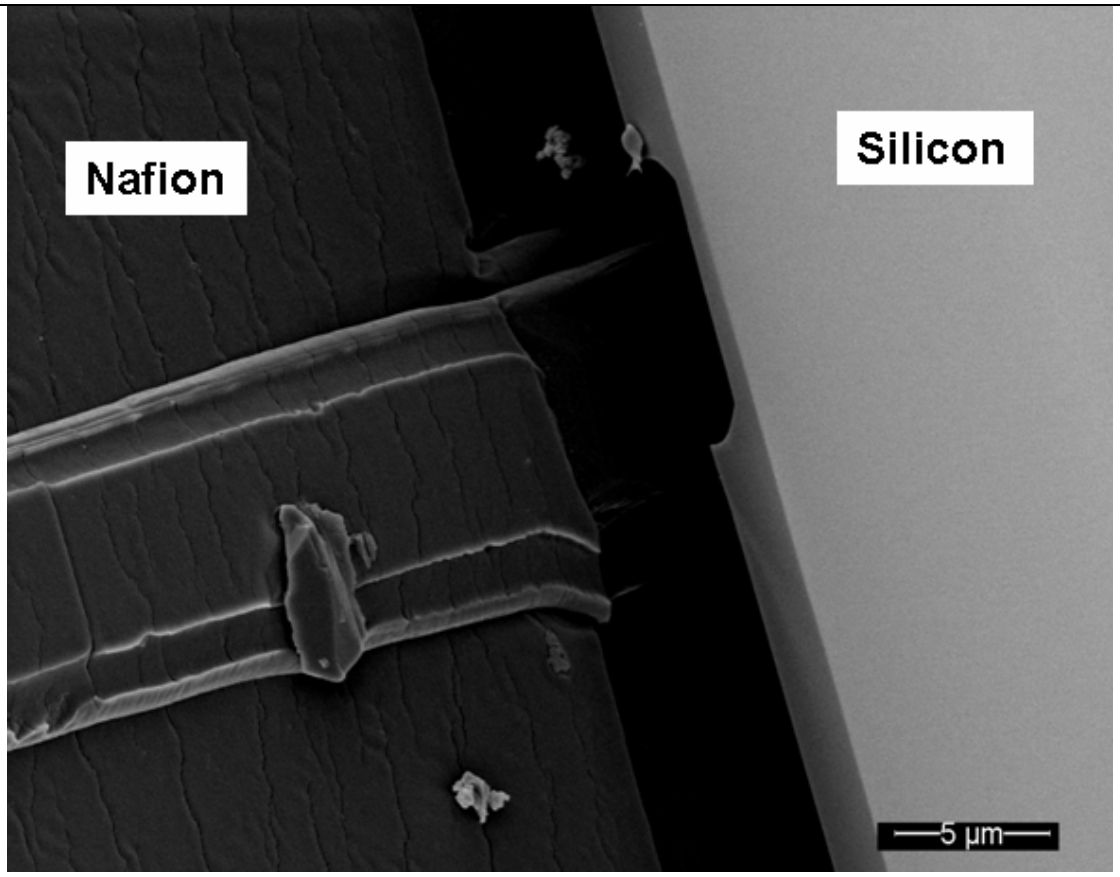

Figure 16: A 3500x magnified SEM image of the Nafion dry-pressed at 90°C. Note that the flat top of the feature indicates that Nafion has deformed all the way into the trench. Also note the continued presence of the horizontal striations.

As can be seen in figure 16, the Nafion that was dry-pressed at 90°C has clearly penetrated into the silicon trenches. The flat top of the Nafion features indicates that the Nafion has not deformed partially into the trench but has instead deformed all the way to the bottom of the trench. Figure 17 shows Nafion that has pulled away from the silicon trenches during the fracturing process. However, the silicon debris that remains on the Nafion clearly shows that the Nafion features have significant height, thus indicating that the Nafion dry-pressed at 90°C

deeply penetrated into the silicon trenches during pressing. This marks a departure from the types of deformation that have been seen at the lower temperatures in which only the outline of the trenches was visible in the Nafion.

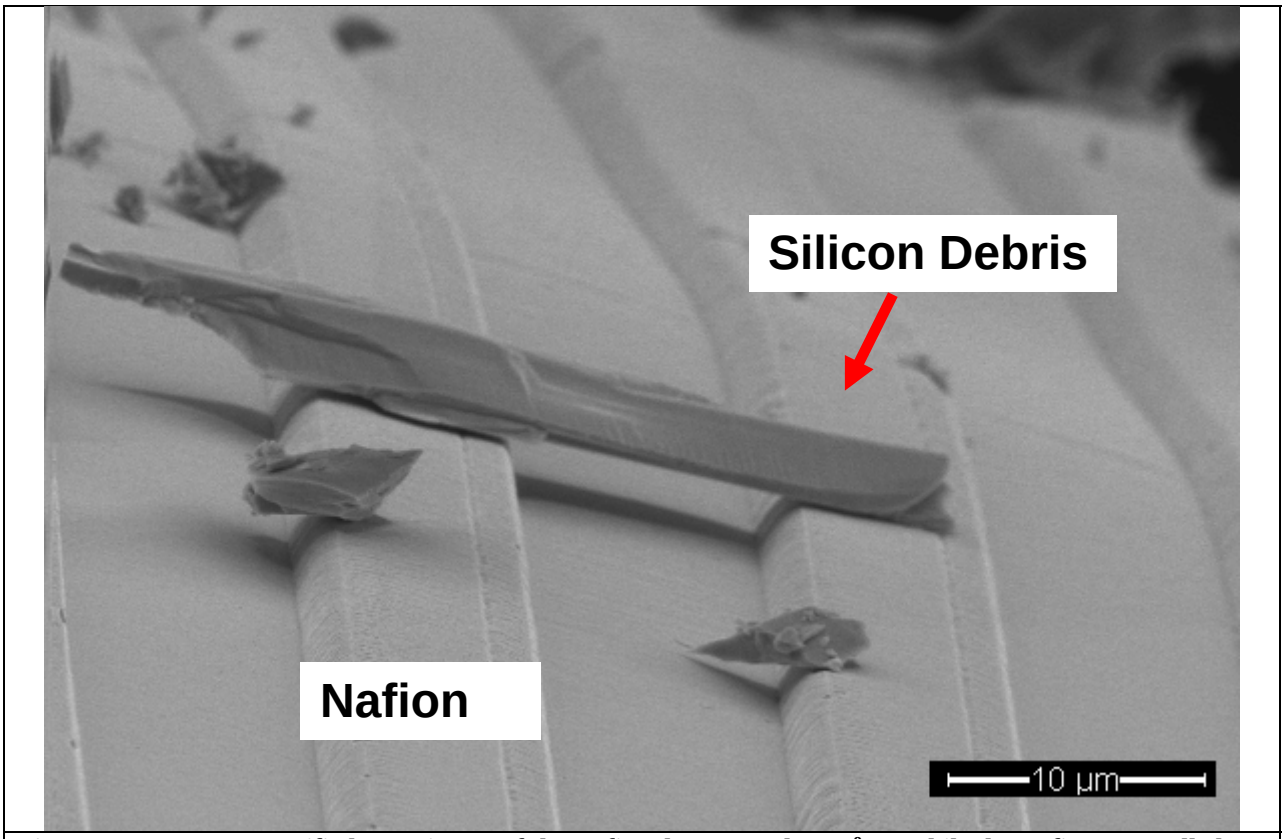

Figure 17: A 2500x magnified SEM image of the Nafion dry-pressed at 90°C. While the Nafion was pulled away from the silicon during fracturing, the remaining silicon debris highlights the height of the Nafion features.

Wet-Pressed

Unlike the Nafion dry-pressed at 90°C, the Nafion wet-pressed at 90°C has not penetrated all the way into the silicon trenches. While the Nafion and silicon have again shifted slightly away from each other during the fracturing process, figure 18 shows that the wet-pressed Nafion deformed significantly less than the Nafion dry-pressed at 90°C. The 90°C temperature is the

first temperature at which a difference in water activity level has led to a significant change in the degree to which the Nafion deforms. While counterintuitive, this result does agree with the results found in the Majsztrik (2007) [5] study, which found that while at 25°C, water does act as a plasticizer, at 90°C water stiffens Nafion.

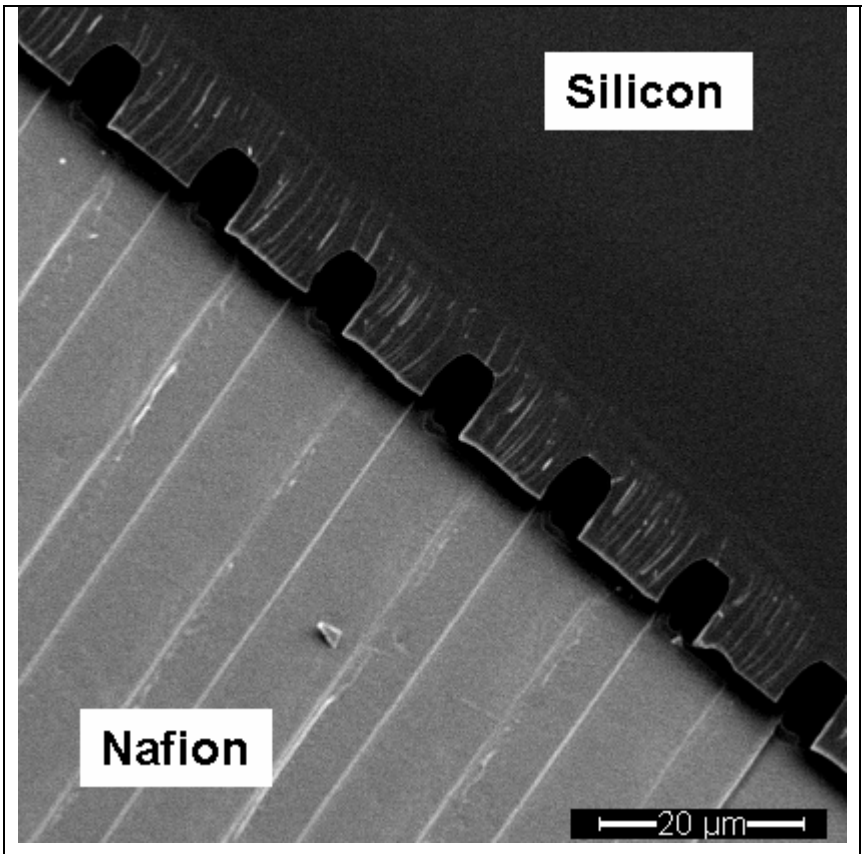

Figure 18: A 1000x magnified SEM image of the Nafion wet -pressed at 90°C. Note that while the Nafion and silicon have shifted slightly away from each other, it is apparent that the Nafion has not completely penetrated the silicon trenches.

While figure 18 shows that the Nafion has deformed to show the outline of the silicon trenches, because of the separation between the silicon and Nafion that arose during fracturing it is difficult to determine the depth of the Nafion features. Figure 19 is another image of the same 90°C wet-pressed sample. While this image shows even more evidence of the damage incurred

during the fracturing process, the silicon debris present on the Nafion acts as a visual aid in determining the depth of the features present in the Nafion. From the silicon particles lying across the Nafion features, it is evident that the Nafion features are shallow, thus showing that during pressing the Nafion deformed only slightly into the 5μm deep trenches.

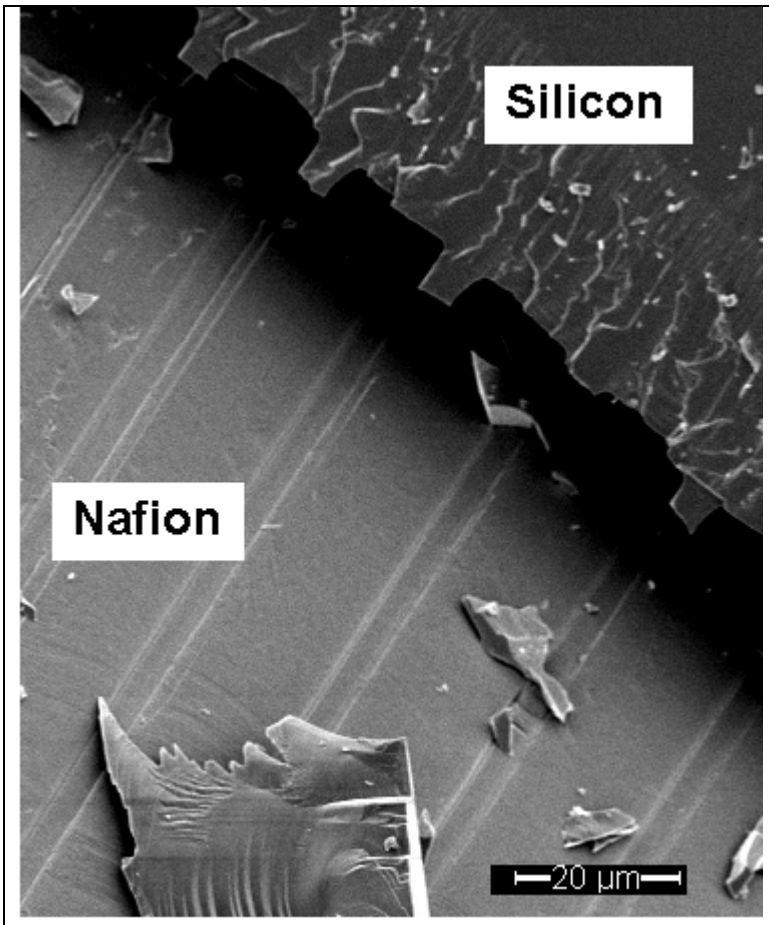

Figure 19: An 800x magnified SEM image of the Nafion wet - pressed at 90°C. Note that while the silicon has been severely damaged during sample preparation, the silicon debris on the Nafion helps show the shallowness of the Nafion features.

4.1.4 Pressing at 120°C

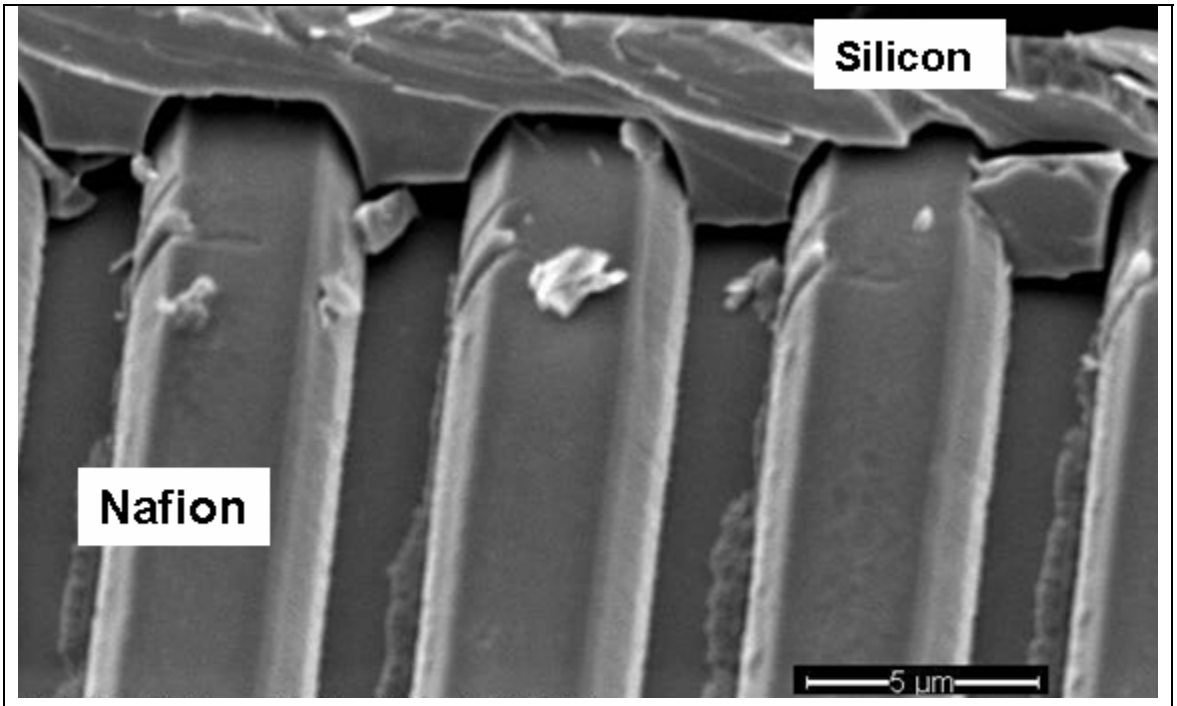

Figure 20: A 5000x magnified SEM image of the Nafion dry-pressed at 120°C. Note that the Nafion has completely deformed into the trenches. Also note that there are no striations present in the Nafion as there were in samples pressed at lower temperatures.

Unlike the samples pressed at lower temperatures, the samples pressed at both 120°C and 140°C retained contact between the silicon substrates and the Nafion even after the freeze fracturing process. This is undoubtedly due to the deeper deformation of the Nafion into the trenches at these higher temperatures and the resulting larger contact area. As can be seen in figure 20, at 120°C the Nafion has completely deformed into the features in the silicon substrate. It is interesting to note that there are no striations present in the Nafion as there were in some samples pressed at lower temperatures. This could imply that the flow of the Nafion into the trenches reduces the stress on the bulk of the Nafion during pressing.

4.1.5 Pressing at 140°C

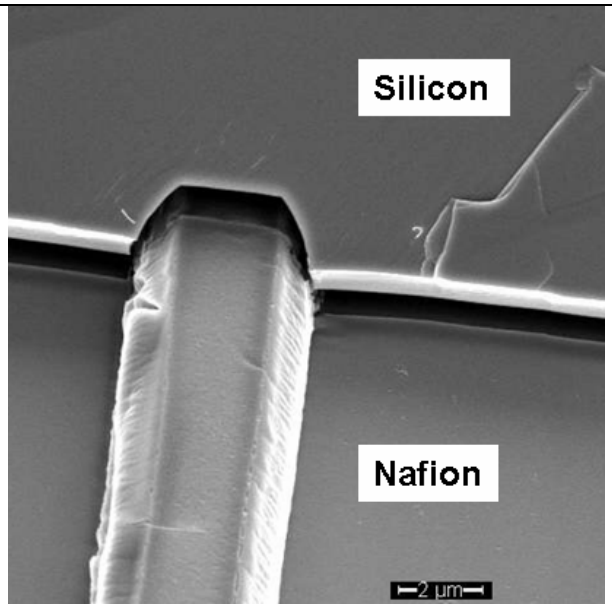

Figure 21: A 6500x magnified SEM image of the Nafion dry-pressed at 140°C. Note that the Nafion has completely deformed into the trench. Also note the lack of any reverse curvature as was observed in the Lehr (2005) thesis.

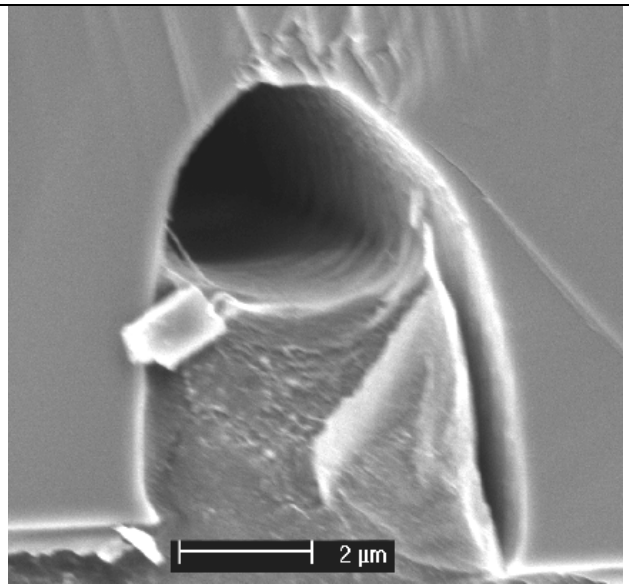

Figure 22: A 9158x magnified SEM image by Lehr (2005) of Nafion dry-pressed at 140°C. The silicon substrate is at the top of the image with the Nafion on the bottom. Note that the curvature in the Nafion that has deformed into the trench is the opposite of the curvature observed at all temperatures in this thesis.

As can be seen in figure 21, the Nafion pressed into the silicon substrate at 140°C has also completely deformed into the trenches. Again, as was the case in the sample pressed at 120°C, there are no striations present in the Nafion. What is interesting about images of the sample pressed at 140°C is the lack of a reverse curvature in the Nafion that had penetrated the trenches. Using the same procedure, Lehr (2005) found that at 140°C Nafion exhibited an unusual reverse curvature in the Nafion features as can be seen in Lehr's image in figure 22. This observation of a reverse curvature at a pressing temperature of 140°C was a major finding of the Lehr 2005 thesis and potentially has important implications for the micro-structural rearrangement of Nafion during the pressing process. The inability to repeat this finding deserves further attention.

4.2 Discussion of Temperature and Hydration Dependence of Deformation

In general, at a constant applied pressure, non-hydrated polymers usually exhibit an increase in deformation as the temperature is increased. This is because at room temperature, there is significant intermolecular bonding, in the case of Nafion it is ionic bonding which impedes relative molecular movement thus effectively limiting overall deformation [16]. As the temperature increases, the kinetic thermal energy of the molecules decreases the amount of intermolecular bonding and polymers are more easily deformed [16]. The behavior of dry Nafion was consistent with this paradigm.

In many polymers, hydration aids deformation by acting as a plasticizer [17]. However, as can be seen from the 90^{o}C pressed results of this thesis, Nafion differs from many polymers in that at high temperatures hydration impedes deformation. As illustrated in figure 23, this has been attributed to the presence of hydronium ions creating stronger crosslinks between sulfonic acid groups within the Nafion [5]. Majsztrik's work interestingly noted that while this stiffening effect of hydration was present at 90^{o}C, water acted as a plasticizer below 50^{o}C. Majsztrik attributed this to an increase in free volume with hydration at low temperatures, which would be consistent with Gierke's cluster-network model. However, this result was not evident in this study due to the limited deformation of both wet and dry Nafion at temperatures below 90^{o}C.

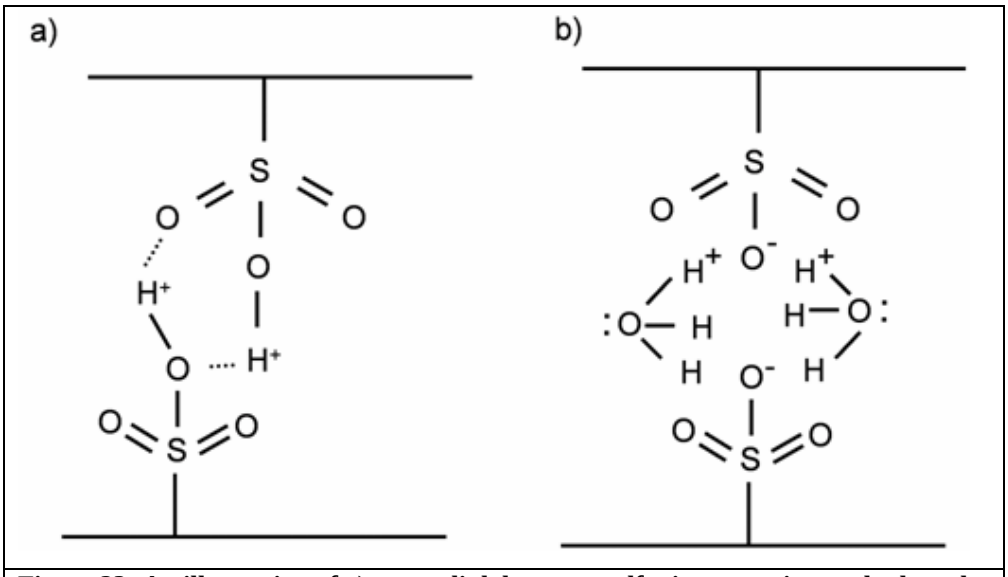

Figure 23: An illustration of a) a crosslink between sulfonic groups in non-hydrated Nafion and b) a crosslink strengthen by a hydronium ion in hydrated Nafion. From Majsztrik 2007 [5].

4.3 Determining the Cause of the Discrepancy in Observation of Reverse Curvature

4.3.1 Testing the Effect of Pressure on Observed Curvature

The discrepancy in observation of a reverse curvature in Nafion pressed at 140^{o}C could be due to the digression in the procedure performed in this study from the Lehr thesis, the pressure at which the samples were pressed. The polymer press used to press the samples together takes force as an input rather than pressure. While Lehr used 2,000lbf of force just as was used in this thesis, the size of the samples Lehr used was quite different. Lehr microfabricated and pressed the entire 3" diameter wafers of silicon and her samples therefore had a surface area of 7.07 in^2. It this study, it was difficult to spin coat an even layer of photoresist over such a large wafer size and the solution employed to ensure consistent photoresist was to cut the wafers into four equally sized wedges. The surface area of the samples when pressed was thus one fourth those in the Lehr thesis, effectively quadrupling the applied

pressure. This four-fold increase in pressure stood as a potential reason for the discrepancy in observation of reverse curvature.

In order to see if this difference in applied pressure during pressing was indeed the cause of the discrepancy in finding a reverse in curvature at 140^{o}C, four of the silicon-Nafion "sandwiches" of the same size and type of those pressed in the rest of this thesis were simultaneously pressed at 140^{o}C. This quadrupled the surface area on which the 2,000lbf of applied force from the press was applied and therefore made the applied pressure the same as that applied in the Lehr 2005 thesis. One of the Nafion-silicon samples was then fractured and viewed with the SEM using the same procedure employed with all previous samples. Figure 24 shows a resulting image.

While the fracturing process has shifted the Nafion away from the silicon as well as damaged the silicon, image 24 nonetheless shows that the Nafion pressed at 140^{o}C has again failed to exhibit the reverse curvature observed by Lehr. Because the same pressure and temperature were used to press this sample as the sample in which Lehr observed the reverse curvature, the discrepancy in findings must have another cause.

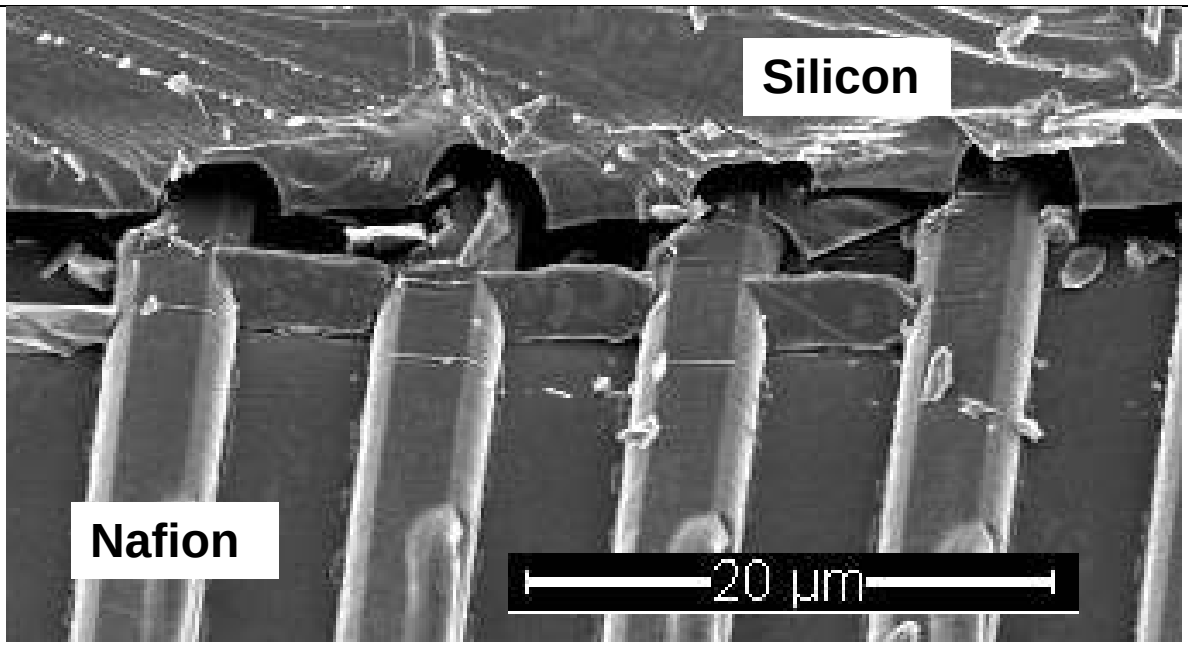

Figure 24: A 1500x magnified SEM image of the Nafion dry-pressed at 140°C with the same applied pressure as the Lehr 2005 thesis. Note that while the silicon has been damaged during the fracturing process, it is still evident that there is a continued lack of any reverse curvature as was observed by Lehr.

4.3.2 Testing the Effect of Relaxation Time on the Nafion Features

Initially, the effect of relaxation time on the features in Nafion that were created during pressing was studied as an aside. Unexpectedly, it quickly became apparent that the work done to study this effect was possibly relevant to explaining the inability to repeat the Lehr finding of a reverse curvature in Nafion pressed at 140°C. As was mentioned in the procedural explanation of this study, all samples were imaged in the SEM the morning after pressing the Nafion and silicon together. Approximately only six hours elapsed between the time the samples were pressed and the time they were viewed in order to minimize the effect of relaxation on the topography of the samples. In order to see the effect of relatively large amounts of relaxation, after their initial viewing, the samples pressed at 120°C and 90°C were placed in an oven left at 90°C and atmospheric pressure for 28 days. The conditions of 90°C and atmospheric pressure

were chosen to mimic the conditions of a fuel cell during operation [1]. After exposure to these conditions for 28 days, the samples were viewed again in the SEM.

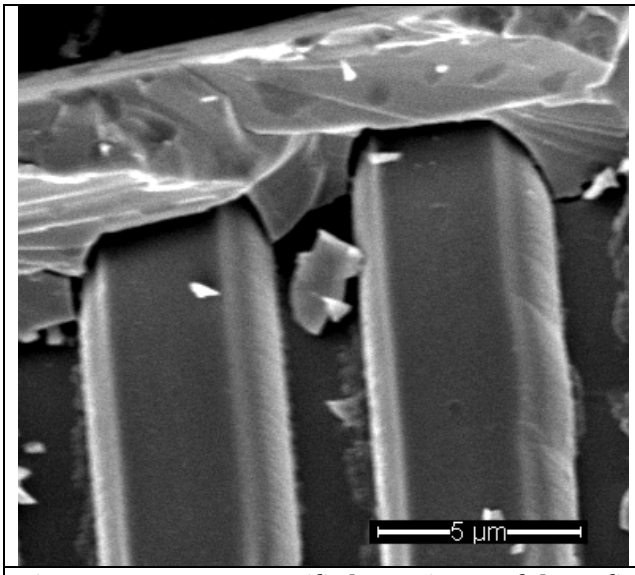

Figure 25: A 5000x magnified SEM image of the Nafion dry-pressed at 120°C. This image was taken approximately 6 hours after pressing.

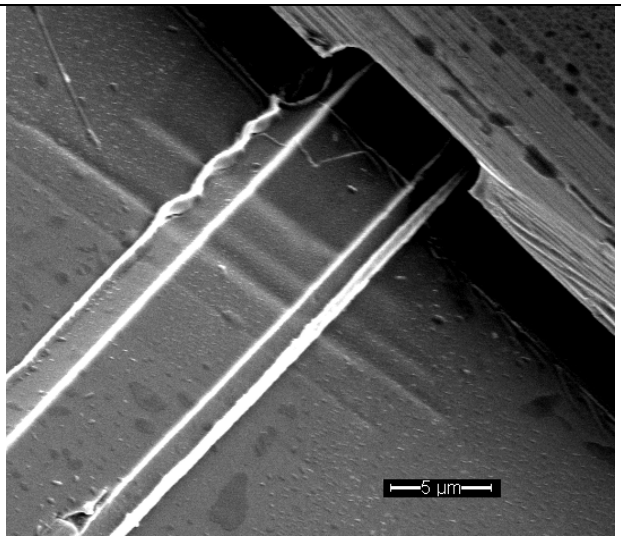

Figure 26: A 3500x magnified SEM image of Nafion dry-pressed at 120°C. This image was taken of the same sample as the image to the left 28 days after pressing. Note that the three orthogonal lines in the Nafion are due to SEM damage that occurred during focusing.

As previously discussed and can be seen in image 25, the Nafion viewed approximately six hours after pressing is still deformed all the way into the silicon trenches. Figure 26 shows an image of the same sample shown in figure 25 but was taken 28 days after the sample was pressed. Figure 26 shows that after 28 days, the Nafion has receded from the silicon and is no longer completely deformed into the trench. Interestingly, it also appears that the curvature of the sides of the Nafion features has reversed from concave in to concave out. Figure 27 is a simplified representation of the change in curvature exhibited by the Nafion 28 days after being pressed. It is worth noting that this same recession of the Nafion and change in curvature was observed in the 90°C dry-pressed sample re-imaged 28 days after pressing.

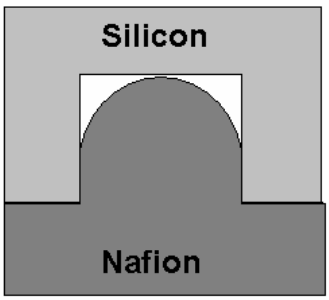

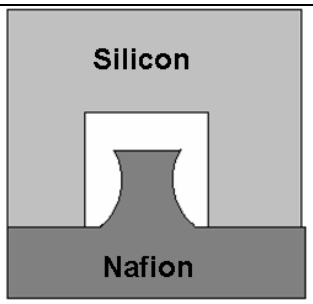

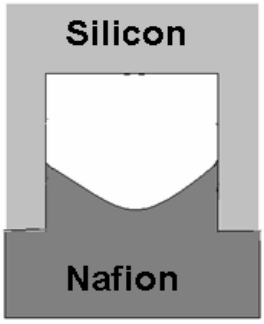

Immediately After Pressing	28 Days After Pressing	Observed in Lehr Thesis

Figure 27: A simplified representation of the Nafion immediately after pressing and 28 days after pressing in this thesis and the Nafion in the Lehr thesis. Note the change in curvature present at the sides of the Nafion feature after 28 days is not exactly the same as the reverse curvature observed by Lehr.

While the change in curvature observed here is different than the reverse curvature observed in the Lehr 2005 thesis, it nonetheless gives insight into what may be the reason behind the reverse curvature Lehr saw. While in this study, the amount of time allowed to elapse between pressing and imaging was held relatively constant at approximately 6 hours, the Lehr 2005 thesis did not specify the amount of time allowed to elapse. This is the only apparent procedural difference between the two studies and might therefore be behind the discrepancy between the observation of a reverse curvature in the Lehr thesis and a lack of such a reverse curvature in this study. This thesis observed a change in curvature of the Nafion features due to relaxation and recovery of the Nafion over a period of several weeks. As can be seen in figure 27 the change in curvature observed here is inherently different than the reverse curvature of the Lehr thesis but it still indicates that relaxation of the Nafion is related to a change in curvature of the Nafion features.

Knowledge that the time between pressing and imaging was not held constant in the Lehr thesis and that the effect of relaxation time on the topography of the pressed Nafion can lead to a

change in curvature leads to the conjecture that the reverse curvature observed by Lehr in Nafion pressed at 140^{o}C was possibly due to relaxation of the Nafion over a prolonged period of time. The difference in the shape of the curvature changes observed in this thesis due to relaxation time and the Lehr thesis might be due to either the amount of time the Nafion was given to recover or the conditions at which the Nafion was stored between pressing and imaging. In the Lehr thesis, the samples were stored for an unspecified amount of time while the "relaxed" sample in this thesis was stored for 28 days. Also, in the Lehr thesis, samples were stored at ambient temperature and humidity while in this thesis the samples were stored at 90^{o}C and 0% relative humidity. The temperature and water activity level of the Nafion greatly affect its rate of deformation and therefore likely also affect the way it recovers from deformation. It is possible that the reverse curvature observed by Lehr was due to an extended period of time the sample was given to recover from deformation induced during pressing.

4.4 The Effect of Pressing Time

In order to determine whether or not the time for which the samples were pressed had a significant impact on the deformation of the Nafion into the trenches, Nafion was dry pressed at 25°C and 50°C for one hour and the resulting deformation was compared to the Nafion pressed at those temperatures for one minute. The temperatures of 25°C and 50°C were chosen because they were the only temperatures at which the dry Nafion did not completely penetrate into the silicon trenches.

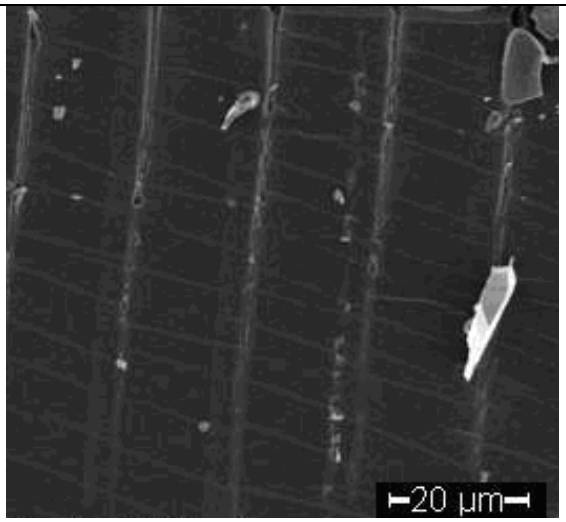

Figure 28: A 650x magnified SEM image of the Nafion dry-pressed at 25°C for one minute.

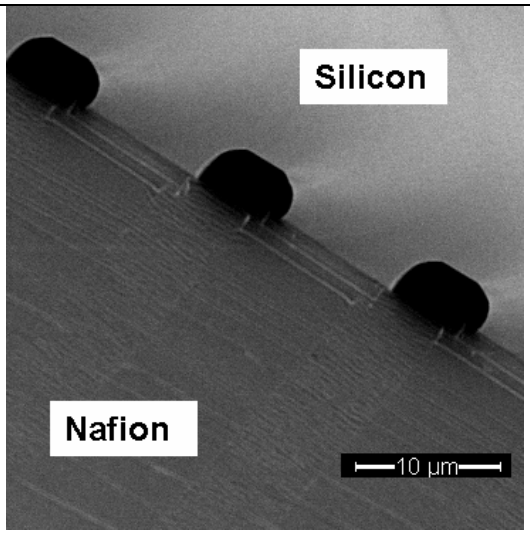

Figure 29: A 2000x magnified SEM image of the Nafion dry-pressed at 25°C for one hour.

Images 28 and 29 respectively show the Nafion dry-pressed at 25°C for one minute and one hour. As can be seen from the images, the Nafion pressed for one hour shows a slightly more defined outline of the silicon trenches. However, the Nafion has still not significantly deformed into the silicon trenches and it appears that at 25°C, the change in the order of magnitude of the pressing time has not had a considerable effect on the deformation of the Nafion.

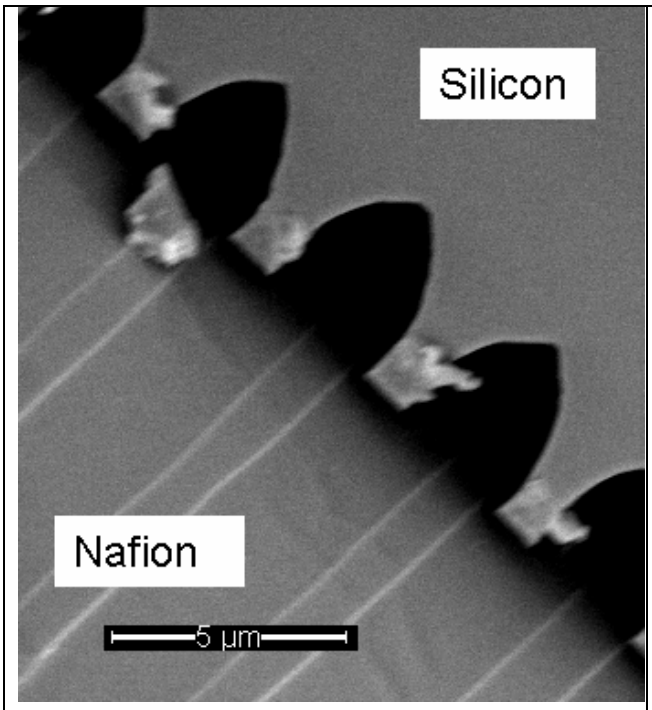

Figure 30: A 5000x magnified SEM image of the Nafion dry-pressed at 50°C. As can be seen from the silicon particle in the upper right hand corner, the features in the Nafion are not very deep.

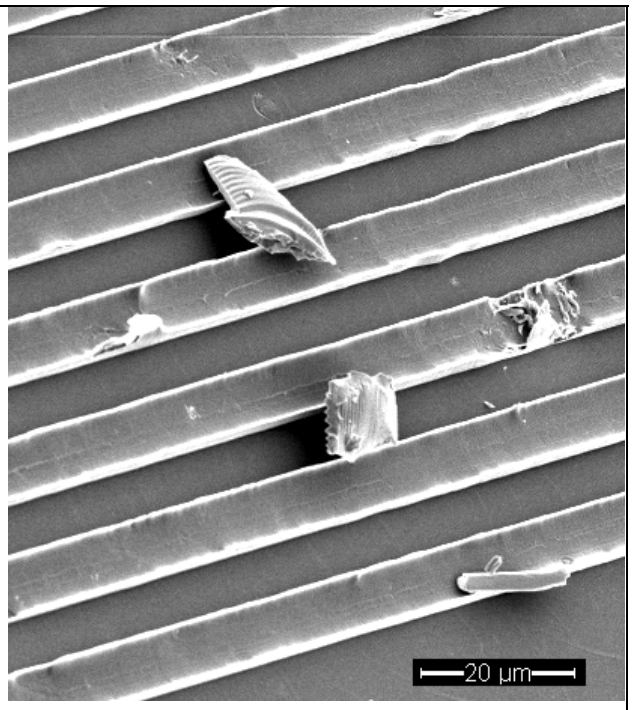

Figure 31: A 1000x magnified SEM image of the Nafion dry-pressed at 50°C for one hour. Note that the particles on the Nafion are silicon and they help show the significant depth of the Nafion features.

Images 30 and 31 respectively show the Nafion dry-pressed at 50°C for one minute and one hour. As can be seen from the images, the Nafion pressed for one hour shows significantly deeper topographical features. This indicates that the increase in pressing time for the Nafion when dry-pressed at 50°C leads to a significant increase in the depth to which the Nafion deforms into the silicon trenches. This result was expected in that creep tests almost exclusively show that deformation increases when the time exposed to stress is increased [18]. When this is compared to the observed effect of pressing time on the Nafion dry-pressed at 25°C, it is evident that the effect of the time of pressing is dependant on the pressing temperature. Once again, it

appears that time and pressing temperature have interrelated effects on the way in which Nafion deforms into the silicon trenches.

4.5 Damage to the Nafion Due to SEM Imaging

While viewing the samples that had been dry pressed at 120 and 140^{o}C, it very quickly became apparent that the samples were extremely susceptible to damage from the incident electron beam of the SEM. The beam used during imaging was 5keV, a standard energy beam for viewing samples of this size and this resolution [13]. The damage that occurred ensued very quickly, within seconds, of focusing the beam on the sample. Figure 32 shows the progression of the damage the beam caused one of the samples over the course of less than three minutes. Image t_1 was the first image taken while all subsequent images were taken approximately 45 seconds apart.

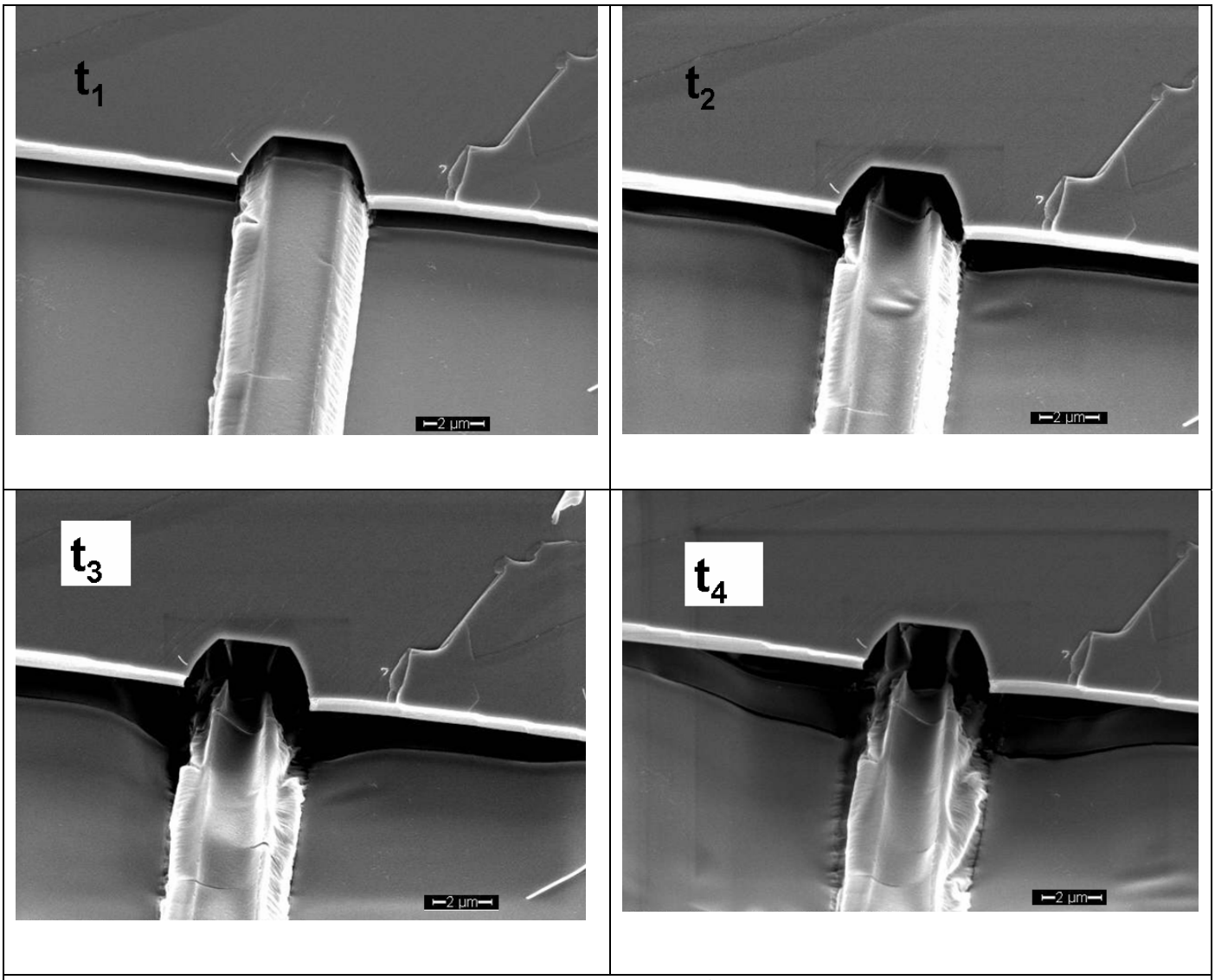

Figure 32: 6,500x magnified SEM images of Nafion dry-pressed at 140°C. Image t_1 was the first image taken while all subsequent images were taken approximately 45 seconds apart with $t_4>t_3>t_2>t_1$. Note the unusual nature of the electron beam damage.

The incident electron beam appears to have damaged the Nafion in such a way that the topographical feature that was once concave down is now concave up. Initially, it was thought that this damage could explain the reverse curvature observed by the Lehr thesis but as can be seen by comparing figures 32 and 22, the features Lehr observed were much more uniform and did not display signs of SEM damage. The damage observed in this thesis seems to indicate that

the beam has preferentially damaged the middle of the Nafion feature rather than the sides of the feature that were at one point in contact with the walls of the silicon trench. What could be the reason for this preferential degradation? The answer to this question can only be found by first understanding the fundamentals of SEM radiation damage.

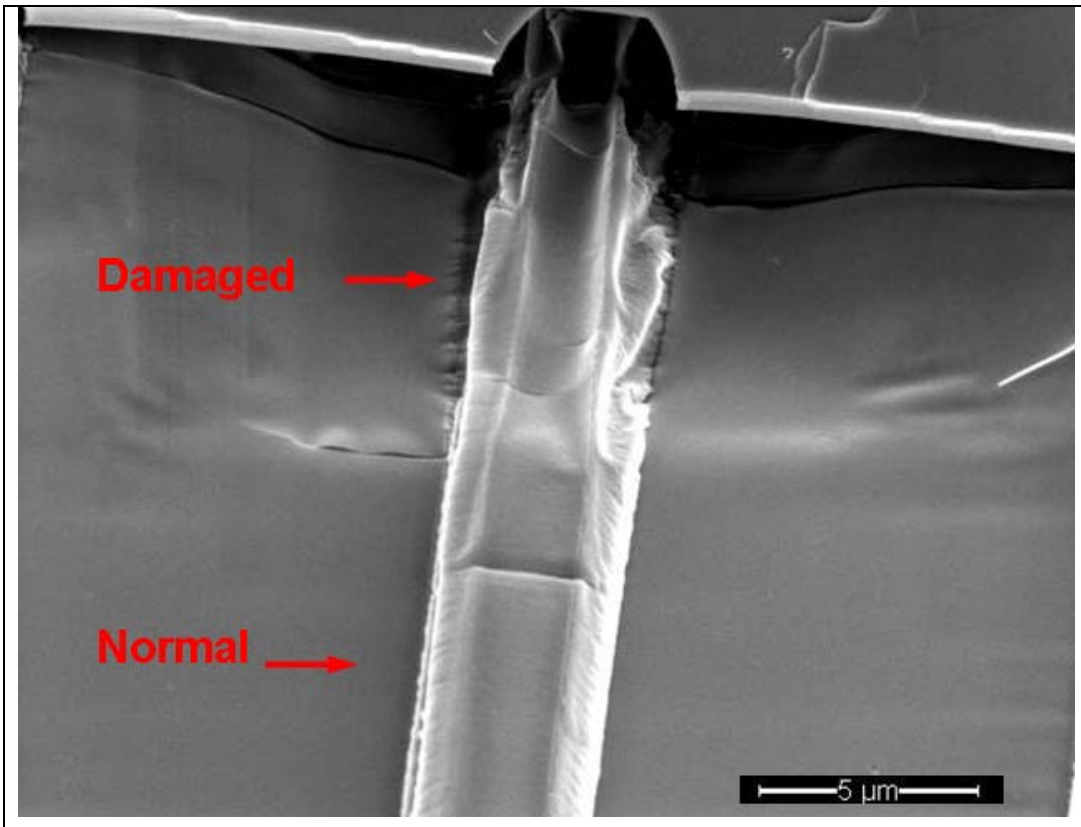

Figure 33: A 5,000x SEM image of both the damaged and undamaged portions of a feature in the Nafion sample dry pressed at 140°C.

Scanning electron microscopes (SEMs) work by focusing a source of electrons on the sample while under vacuum [13]. As the electrons collide with the surface of the sample, a number of interactions take place that ultimately result in the emission of electrons from the surface that are then collected by a detector and used to generate an image. The images in this

thesis were generated using secondary electrons, the electrons that are emitted from the surface of the sample after undergoing inelastic collision with the incident electrons. The incident beam can cause damage to the sample in a number of ways such as electron beam sputtering, electron beam heating, and electrostatic charging [14]. However, based on the images generated, it appears that the most likely culprit for the damage seen here is radiolysis, the electron beam degradation due to inelastic collision of the incident beam. In radiolysis, the incident beam sends an electron from a molecule into a temporary excited state but the subsequent de-excited state of the electron is not necessarily the original electronic state in the original molecule [14]. In this way, radiolysis breaks chemical bonds and changes the overall structure and position of samples that are being viewed.

The susceptibility of a sample to radiolysis must then be dependant on the microstructure of the substance being viewed. The preferential degradation observed in the 120^{o}C and 140^{o}C dry pressed samples might therefore imply that the middle of the Nafion features have a different microstructure than the edges of the feature that were in contact with the Nafion. However, the question then becomes why would the outer and inner portions of the Nafion feature have differing microstructures? The answer to this question might potentially lie in the fact that Nafion is comprised of both hydrophilic (the sulfonic acid groups) and hydrophobic (the TFE backbone) regions. The silicon substrates into which the Nafion was pressed had hydrophilic surfaces and the Nafion could have potentially undergone a rearrangement during the pressing process in which the sulfonic acid groups were on the outside, in contact with the silicon, while the TFE portions were kept more internal to the Nafion structure. This hypothetical rearrangement is illustrated in figure 34.

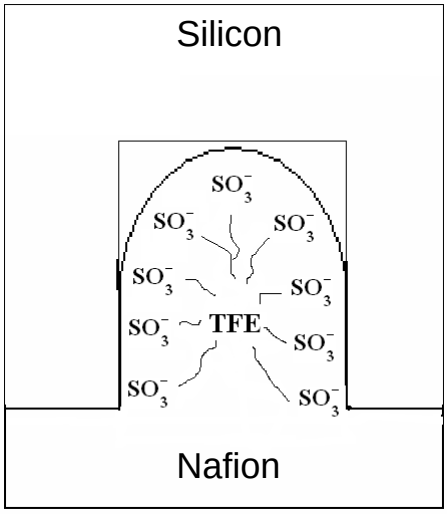

Figure 34: An illustration of the hypothetical restructuring of Nafion in the silicon trenches.

While this explanation of a microstructural rearrangement seems to fit nicely, there are a few other possible explanations for the preferential SEM damage that are worthy of investigation. Perhaps the geometry of the Nafion features is what ultimately made the structures susceptible to such unusual damage? This hypothesis was tested by taking Teflon, a polymer related to Nafion but lacking the hydrophilic sulfonic groups, and pressing it into the same silicon substrates at the same conditions.

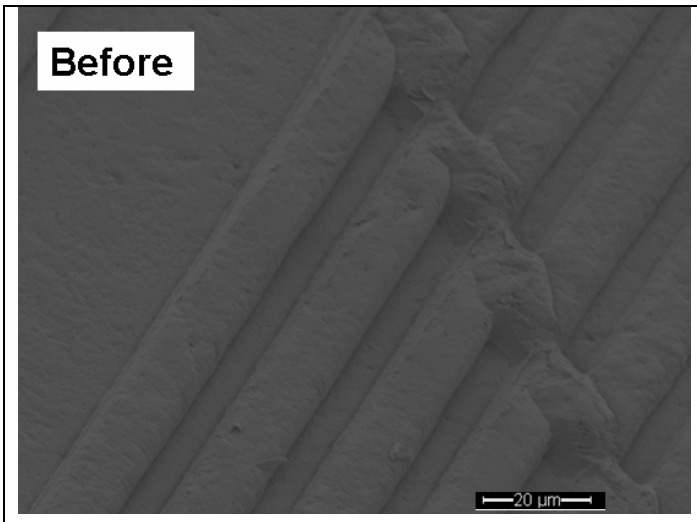

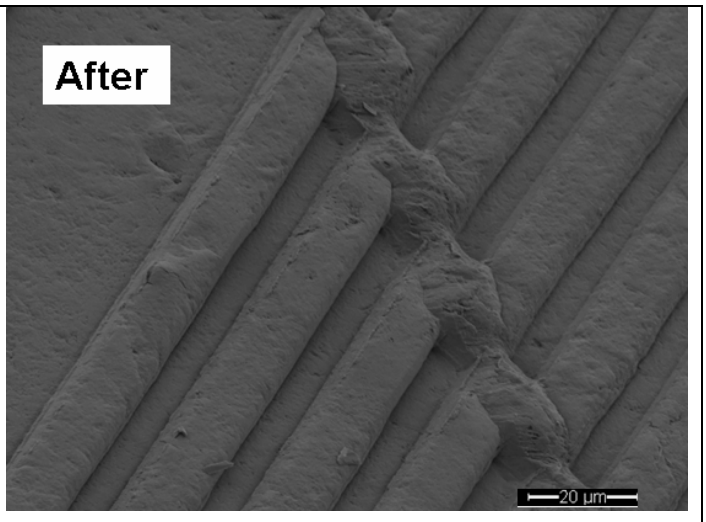

Figure 35: 1000x SEM images of Teflon that was dry-pressed into the silicon substrates at 120°C. The "Before" image shows the initial, unfocused image taken while the "After" image shows the focused image that was exposed to a 25keV incident electron beam for 10 minutes. Note the lack of damage.

The initial image of the resulting Teflon sample was immediately taken, prior even to focusing which requires leaving the incident beam on the sample for several seconds. Several additional images of the sample were then taken over various periods of time. As can be seen in the "After" photo of figure 35, the Teflon was not damaged even after exposure to a 25keV incident electron beam for 10 minutes. This result rules out the geometry of the sample as the root cause of the preferential damage found in the 120^{o}C and 140^{o}C dry pressed Nafion samples. However, this result seems to defy the microstructural rearrangement explanation for the phenomenon as well. If an abundance of the TFE backbone in the center of the sample was what caused the center of the Nafion feature to be preferentially damaged, then Teflon, which is structurally and chemically very similar to the TFE backbone should also have shown extreme susceptibility to damage from the beam.

Perhaps this indicates that the Nafion has restructured itself during deformation such that the sulfonic acid groups are in the center of the feature and the TFE backbone is primarily along the silicon interface? While this explanation would explain the pattern of SEM damage observed, it is contradicted by the fact that the silicon substrate is hydrophilic and the TFE backbone of Nafion is hydrophobic, meaning that a rearrangement of Nafion to lower the surface energy would result in the TFE backbone not being in contact with the silicon. Clearly this pattern of SEM damage needs further investigation before the real reason for its occurrence is uncovered. However, the further investigation of this phenomenon seems very worth while in that it may help uncover knowledge of the microstructural arrangement of Nafion at the Nafion-catalyst interface in fuel cells, which in turn would have important implications for hydrogen transport and fuel cell efficiency.

5. Conclusion

5.1 Concurrence with the Majsztrik (2008) Study and Implications

This thesis examined the deformation of Nafion into trenches that had been microfabricated in silicon to mimic the catalyst layer of a PEM fuel cell. The effects of temperature, water activity level, and time on the manner and extent of this deformation were studied. The original motivation for this thesis was the Benziger at al. (2004) work and the Lehr (2005) thesis that conjectured that a delayed, unexpected jump in generated current of a fuel cell was due to an increase in contact between the Nafion membrane and the catalyst layer as the water content of the Nafion increased. The motivation to examine the effect of pressing temperature along with water activity level came from the Majsztrik (2007) work that studied the synergistic effects of temperature and water activity on the tensile strain of Nafion and unexpectedly found that at 25^{o}C an increase in water activity level increases the creep while at 90^{o}C an increase in water activity level decreases creep.

In this thesis, both the wet and dry samples pressed at 27^{o}C showed only negligible deformation. While neither the wet nor dry samples pressed at 50^{o}C penetrated significantly into the trenches, the wet-pressed Nafion exhibits deeper and more defined outlines of the trenches which indicates that that at 50^{o}C hydration slightly aids Nafion's deformation. The dry sample pressed at 90^{o}C deformed completely into the trenches, while the wet sample pressed at 90^{o}C deformed only partially into the trenches. The results of this thesis could not support the Majsztrik findings at 25^{o}C because the deformation of the dry and wet samples were too slight to be compared. However, the results from the samples pressed at 50^{o}C and 90^{o}C are consistent with the Majsztrik work in that the sample dry-pressed at 90^{o}C deformed significantly further into the trenches than the wet-pressed sample. As expected, the results of this thesis also agree

with the Majsztrik (2007) study in that an increase in pressing time was associated with an increase in deformation. Figure 36 illustrates the main similarities between the results of this thesis and the Majsztrik (2007) work.

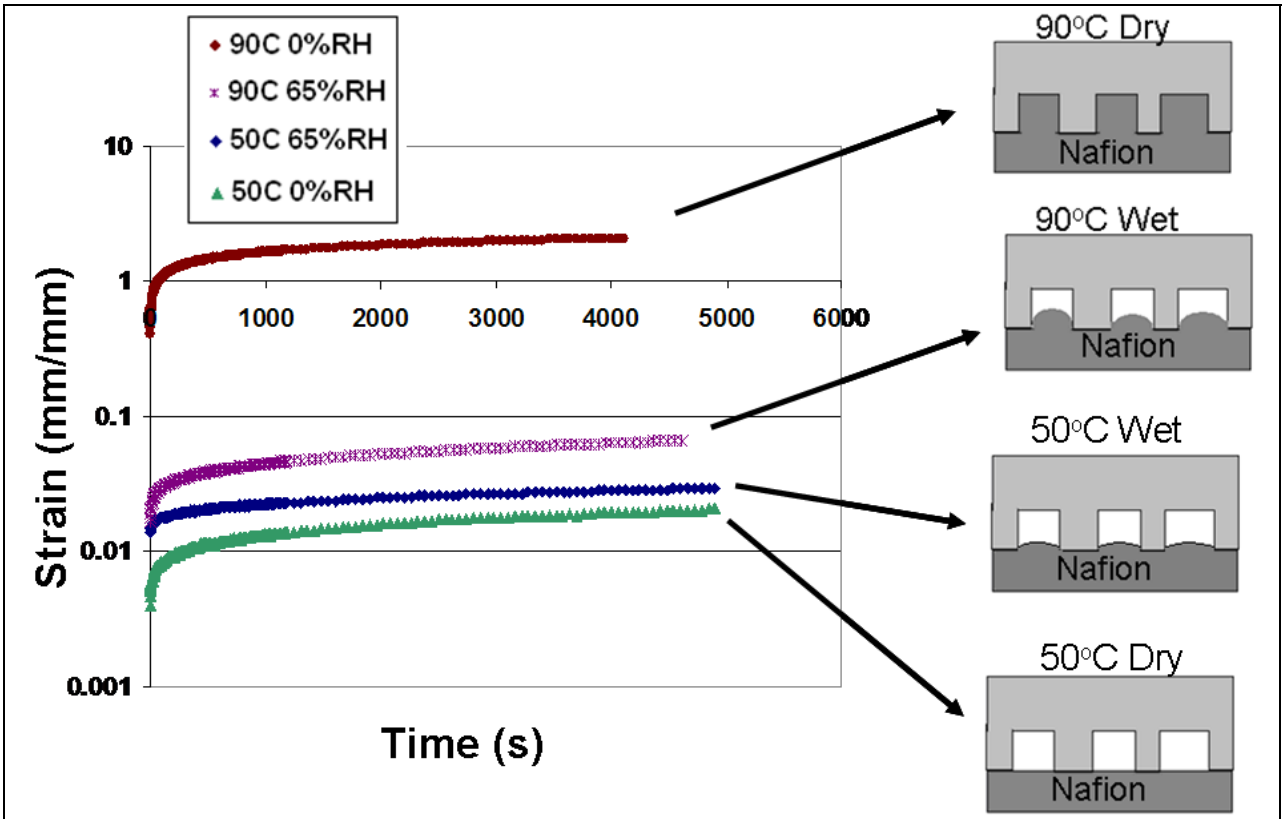

Figure 36: Graph from the 2007 Majsztrik [5] work and illustrations of the results of this thesis. Note that in general the results agree. Also note that the y-axis is logarithmic.

The agreement between the results of the 2007 Majsztrik study [5] and this thesis indicates that the tensile creep tests performed by Majsztrik are strongly correlated to the degree to which Nafion deforms into micro-trenches. If the underlying assumption of this thesis is valid, that the silicon micro-trenches are a valid model of a PEM fuel cell catalyst layer, then the creep tests performed by Majsztrik could be used to predict the conditions in which Nafion will significantly deform into the catalyst layer. If the conjecture put forth in Benziger et al.(2004) [3], that the deformation of Nafion into the catalyst layer increases the current output, is true,

then the creep tests performed by Majsztrik could be a useful tool in helping determine the optimal conditions for fabrication and operation of a fuel cell. While contact between the catalyst layer and the Nafion is only one of many parameters that determine fuel cell performance, it is still very much worth considering.

5.2 Dissension from the Lehr (2005) Thesis and Implications

The results of this thesis are consistent with several results of the Lehr (2005) thesis [4], namely that as the temperature of pressing increases, the deformation of dry Nafion also increases. However, the findings in this thesis contrasted those found by Lehr in regards to the observance of a reverse curvature in the Nafion that penetrated in the trenches when pressed at 140^{o}C. Even after controlling for a difference in pressing pressure, this thesis was not able to replicate Lehr's finding of a reverse curvature. However, a different type of curvature change was seen in Nafion that was given 28 days of recovery time after pressing. While the curvature observed in the relaxed Nafion was not the same as that observed in the Lehr thesis, it shows that recovery from stress can lead to a structural change in Nafion. This finding has twofold importance. It indicates that perhaps the reverse curvature observed by Lehr was due to an extended period of time the sample was given between pressing and viewing, which is not ruled out by Lehr's procedural write up. Also, this finding indicates that the conditions at which the fuel cell operates may be just as important in determining the nature of the catalyst-Nafion interface as the conditions at which it is fabricated.

5.3 SEM Damage and Micro-structural Implications

The Nafion pressed into the silicon trenches at 120^{o}C and 140^{o}C was found to be highly susceptible to damage from the incident electron beam in the SEM. Perhaps more noteworthy was the unusual manner in which the beam preferentially damaged the center of the Nafion features while leaving the outer surfaces of the features, which had been in contact with the silicon trenches, relatively intact. It is conjectured that the incident electron beam degraded the Nafion by breaking chemical bonds within the polymer through the process of radiolysis. This would imply that the microstructure and chemical composition of the surface of the Nafion in contact with the silicon differed from that of the bulk Nafion.

Teflon, which is a polymer similar to the TFE backbone of Nafion, was not degraded by the SEM incident electron beam. This would indicate that the Nafion in the 120^{o}C and 140^{o}C pressed samples had rearranged such that the hydrophobic TFE segments of the polymer were in contact with the silicon. However, this is most likely not the case because the surface of the silicon trenches is hydrophilic, thus meaning that a rearrangement of the polymer to lower the surface energy would have put the sulfonic acid groups of the polymer in contact with the silicon rather than the TFE segments. Clearly this degradation phenomenon needs to be studied further before it can be fully explained. However, while it cannot be accounted for, the unusual degradation of the Nafion is noteworthy in that it implies that a micro-structural rearrangement of the Nafion takes place along with the macro-structural deformation into the trenches. This effect could have major implications for transport phenomena occurring at the Nafion-catalyst interface in a fuel cell and is therefore worth further examination.

5.4 Recommendations for Further Study

It would be useful to obtain results of a more quantitative nature on the degree to which Nafion deforms into the silicon trenches under various pressing conditions. This could be done by following the procedure performed in this thesis but rather than using an SEM to view the Nafion-silicon interface, an atomic force microscope (AFM) could be used to obtain the profile of the deformed Nafion. An AFM generated profile would precisely and accurately yield the distance that the Nafion deformed into the silicon trenches.

It goes without saying that the nature of an interface is dependant at least partially on the identity of all of the components present at the interface. While the Nafion membrane studied in this thesis is the same membrane used in fuel cells, the idealized model of the catalyst layer employed was made of silicon rather than carbon and platinum, the components of the catalyst layer in a real fuel cell. The interface between the Nafion and the catalyst layer in a real fuel cell might therefore show a different dependence on temperature and water activity level than what was observed in the idealized model used in this thesis. It would be useful to perform this study again by pressing Nafion at various temperatures and water activity levels into a real catalyst layer and then freeze fracturing and imaging the resulting interface.

One of the major limitations of this study was the inability to control relative humidity of the Nafion during pressing. Therefore, only two "water-activity levels" could be examined: completely soaked in water and ambient humidity. In order to understand the effect of water activity level on Nafion deformation in more detail, it would be useful to press the Nafion and silicon in a humidity controlled environment.

The largest unanswered question resulting from this study stems from the unexplained preferential damage to the Nafion features by the incident electron beam of the SEM. While it

implies some sort of micro-structural rearrangement of the Nafion, the exact resulting microstructure is unknown. The chemical composition of the surface of the Nafion features could most likely be determined by energy dispersive X-ray spectroscopy (EDX). EDX would generate the ratio of sulfonic acid groups to TFE units by showing the relative number of every element present at the surface [19]. From this ratio, it could be determined if the Nafion had deformed such that mostly sulfonic acid groups or TFE were in contact with the silicon trenches.

Finally, the samples that were given 28 days of recovery time between pressing and viewing indicated that, in addition to the fabrication conditions, the operating conditions of a fuel cell are also parameters that determine the nature of the Nafion-catalyst interface. However, much more work needs to be done on understanding the exact way operating conditions affect this interface. The procedure performed in this study could be repeated with the pressing conditions held constant and then varying both the temperature and water activity level the Nafion is stored at, as well as the amount of time it is stored at these conditions, prior to viewing.

References

1. Barbir, F., *PEM Fuel Cells*. 2005, Amsterdam: Elsevier Academic Press.
2. Larminie, J. and A. Dicks, *Fuel Cell Systems Explained*. 2003, West Sussex, England: John Wiley & Sons Ltd.
3. Benziger, J., et al., *The Stirred Tank Reactor Polymer Electrolyte Membrane Fuel Cell*. AIChE Journal, 2004. 50(8): p. 1889-1900.
4. Lehr, A. BSE Thesis, Princeton University. 2005.
5. Majsztrik, P. PhD Dissertation, Princeton University. 2008.
6. IUPAC, *Glossary of Basic Terms in Polymer Science*. Pure and Applied Chemistry, 1996. 68(8): p. 1591-1595.
7. Banerjee, S. and D. Curtis, Nafion *Perfluorinated Membranes in Fuel Cells*. Journal of Fluorine Chemistry, 2004. 125:p. 1211-1216.
8. Heitner-Wirguin, C., *Recent Advances in Perfluorinated Ionomer Membranes*. Journal of Membrane Science, 1996. 120:p. 1-33.
9. Yeo, S.C. and A. Eisenberg, *Physical Properties and Supermolecular Structure of Perfluorinated Ion-Containing (Nafion) Polymers*. Journal of Applied Polymer Science, 1977. 21: p. 875-898.
10. Gierke, T.D., G.E. Munn, and F.C. Wilson, *The Morphology in Nafion Perfluorinated Membrane Products, as Determined by Wide- and Small- Angle Xray Studies*. Journal of Polymer Science: Part B: Polymer Physics, 1981. 19: p.1687-1704.
11. Yeager, H.L. and A. Steck, *Cation and Water Diffusion in Nafion Exchange Membranes: Influence of Polymer Structure*. Journal of the Electrochemical Society, 1981. 128(9): p. 1880-1884.
12. Delly, J., *Light Microscopy*. Encyclopedia of Materials Characterization: Surfaces, Interfaces, Thin Films, ed. Brundle, R. and C. Evans. 1992, Greenwich: Manning Publication Company.
13. Bindell, J. *Scanning Electron Microscopy*. Encyclopedia of Materials Characterization: Surfaces, Interfaces, Thin Films, ed. Brundle, R. and C. Evans. 1992, Greenwich: Manning Publication Company.

14. Egerton, R., et al., *Radiation Damage in the TEM and SEM*. Micron, 2004. 35:p. 399-409.

15. ECEn Dept. Web Team, Brigham Young University Department of Electrical *Engineering. Reactive Ion Etching Basics*. <http://www.ee.byu.edu/cleanroom/rie_etching.phtml.> Accessed April 14th, 2008.

16. Daniels, C. A., *Polymers: Structure and Property*. 1989, Lancaster: Technomic Publishing Company, Inc.

17. Levine, H., and L. Slade, *Water as a Plasticizer: physico-chemcial aspects of low-moisture polymeric systems*. Water Dynamics, ed. Franks, F. 1988, Cambridge: Cambridge University Press.

18. Ferry, J. D., *Viscoelastic Properties of Polymers*. 1980, New York: John Wiley & Sons Ltd.

19. Russ, J. C., *Fundamentals of Energy Dispersive X-Ray Analysis*. 1984, Kent, England: Butterworths.